We are IntechOpen, the world's leading publisher of Open Access books Built by scientists, for scientists

6,900
Open access books available

186,000
International authors and editors

200M
Downloads

Our authors are among the

154
Countries delivered to

TOP 1%
most cited scientists

12.2%
Contributors from top 500 universities

WEB OF SCIENCE™

Selection of our books indexed in the Book Citation Index in Web of Science™ Core Collection (BKCI)

Interested in publishing with us?
Contact book.department@intechopen.com

Numbers displayed above are based on latest data collected.
For more information visit www.intechopen.com

Chapter 4

Internal Crystallisation Method to Produce Oxide Fibres and Heat Resistant Composites

Sergei T. Mileiko

Additional information is available at the end of the chapter

http://dx.doi.org/10.5772/61024

1. Introduction

Most efforts in developing advance materials to be used in machines for transportation and power generation have been always directed towards enhancing the energy efficiency of the machines, which means decreasing fuel consumption per a unit of useful work. Researchers all over the world have done a lot to reach the goal including developing structural materials with higher specific characteristics to enhance the ratio of a payload to weight of the structure, improving aerodynamics, applying appropriate coatings on hot details, cooling them, etc. However, enhancing the use temperature of structural materials for hot parts of machines has been and will be always a most efficient way to improve the energy efficiency of transportation and power generation.

Most heat resistant materials for heavily loaded structural elements, those being Ni-based superalloys are approaching their physical limit set by their microstructural stability and melting points. Perhaps, this limit will be around 1100°C and a dependence of the maximum use temperature on year of the alloy development is asymptotically going to this limit.

The importance of developing heat resistant material beyond nickel superalloys can be clearly demonstrated by comparing the history of enhancing the use temperature of superalloys and the history of developing aviation jet engines expressed in fuel efficiency of them. Both histories are presented in Figure 1.

At present, at least three families of heat resistant materials of an enhanced use temperature are developing:

1. Ceramic matrix composites (CMCs);
2. Metal matrix composites (MMCs);

INTECH
open science | open minds

© 2015 The Author(s). Licensee InTech. This chapter is distributed under the terms of the Creative Commons Attribution License (http://creativecommons.org/licenses/by/3.0), which permits unrestricted use, distribution, and reproduction in any medium, provided the original work is properly cited.

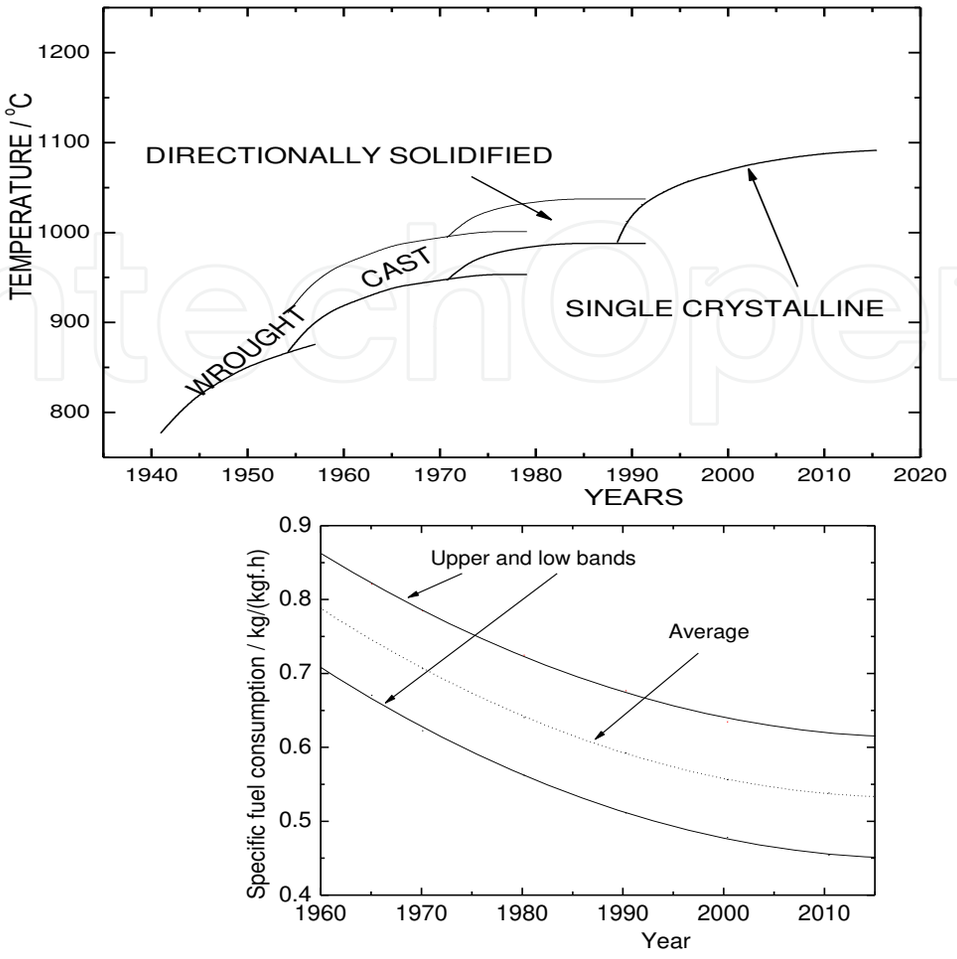

Figure 1. The growth of the use temperature of nickel superalloys [1] and decreasing the specific fuel consumption of aviation engines [2] with the time of their developing. The use temperature is determined by rapture stress 150 MPa at 1000 h.

3. Refractory metal alloys.

Active development of CMCs started with works by R. Naslain [3] and has now reached a stage of the active implementation [4]. The main efforts in this direction have been focused on silicon-carbide-fibres/silicon-carbide-matrix composites certainly due to a higher creep resistance of SiC fibre as compared to polycrystalline oxide fibres. Still, oxide/oxide composites have been developing to occupy an appropriate niche [5, 6, 7].

Metal matrix composites occur now to be in shadow of CMCs; however, it will be shown in this chapter that they have quite prospective future provided a number of the problems are solved.

The mainstream in the development of refractory metal alloys is alloying the matrix by silicon and some refractory metals to form complex silicides particles in the matrix. The main problem in the development of such alloys is to tailor their microstructure to reach an appropriate balance between creep resistance, fracture toughness and resistance to gas corrosion of the

http://dx.doi.org/10.5772/61024

material to satisfy strict requirements set by the loading and heating conditions of a gas turbine blade surrounded by combustion products containing oxygen. Modern niobium alloys [8, 9], unlike those developed earlier [10] are characterized by high fracture toughness and oxidation resistance, which certainly allows using them at temperatures up to about 1200°C.

A further enhancement of the use temperature of heat resistant materials will be, perhaps, possible by appropriate tailoring molybdenum-based alloys. The present mainstream in this direction is developing alloys in the Mo-Si-B system [11]. Despite an essential enhancement of gas corrosion resistance of such alloys as compared to well-known molybdenum alloys [12], the balance between creep resistance and fracture toughness does not seem to have been reached yet [13].

A fundamental difference between metal alloys and metal matrix composites is a correlation between strength and fracture toughness of these two types of structural materials. Strengthening metal alloys, as a rule, limits dislocation movements and, hence, decreases crack resistance; reinforcing metal matrix with high strength **brittle** fibres yields obviously an increase in the strength and can yield an increase in the fracture toughness at the same time [1]. Therefore, development of MMCs promises better results than that of metal alloys.

To go on with the development of heat resistant MMCs, now some scientific and technical problems should be solved. Fabrication technology of appropriate fibres and composites with sufficiently high oxidation resistance are among the most important problems. The present chapter is to focus mainly on these items. We start with oxide fibres of single crystalline and eutectic structures and then proceed with discussing MMCs containing such fibres. Finally prospects of the internal crystallysation method to obtain new types of fibres and composites will be briefly discussed.

2. Fundamentals of the internal crystallisation method (ICM)

The only way to produce either single crystalline oxides or those with typical eutectic microstructure is to crystallize oxide melts. Three main methods to crystallise such fibres are well known:

1. Edge Feeding Growth (EFG);
2. μ-pulling down (μ-PD);
3. Laser heated pedestal growth (LHPG).

EFG was used to produce sapphire fibres for the first time by LaBelle and Mlavsky [14]. The method can actually be positioned within a concept of crystallising a melt by using a shaper formulated by Russian scientist Stepanov before the WWII [15]. Stepanov introduced a shaper to pre-determine a shape and size of the capillary column at the top of which the liquid/solid interface arises (Figure 2). Both a review of the corresponding techniques and discussion of the fibre growth parameters, structure and mechanical properties of sapphire fibres are presented in a paper dated by 1985 [16]. It appears that a stable growth takes place at rates of

no higher than 0.5 - 1.0 mm/s, which makes productivity rate of the process low, so that the cost of the fibres is too high to use them in structural applications. The macrostructure and strength of sapphire fibres depend strongly on the crystallization rate.

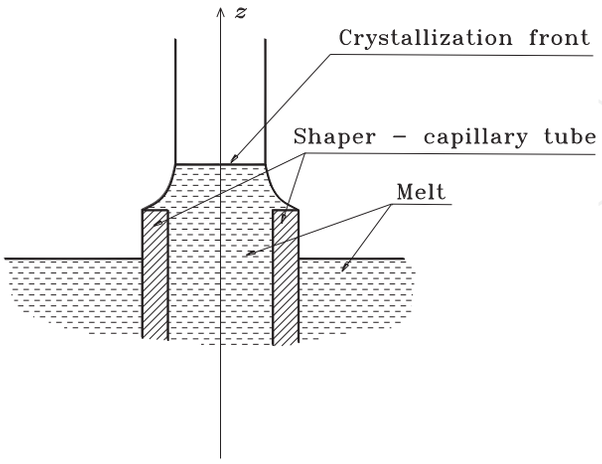

Figure 2. Capillary shaping-crystallization zone, a schematic view of Stepanov's concepts.

Developers of μ-PD method, Japanese researchers [17], did actually turn up down a classical scheme of EFG, which simplified slightly growth procedures. They claim that the usage of the μ-PD yields crystals with smaller thermal strains compared to other growth methods and using this method makes possible to grow crystals even from incongruent melts. Still, the method does not allow an essential decrease in the fibre cost as compared to EFG.

LHPG was used, perhaps for first time, to grow single-crystal Cr-doped Al_2O_3 fibres from a small source rods melted locally on its end by a CO_2 laser [18]. Then it has been used rather intensively to grow mainly optical fibres [19], although attempts to grow structural fibres are also known [20]. There are some advantages of the method: the absence of a crucible allows growing sufficiently pure crystals; a small volume of the melts yields an increase in both thermal efficiency despite of a low efficiency of the laser heating and and mass exchange around the process zone that would be useful in growing such materials as mullite, which is characterized by a complicated phase diagram.

The methods just described have been used to produce continuous oxide fibres of high quality, which are effectively used in various non-structural applications (laser optics, sensors, scintillations, etc.). At the very beginning of the composite era, in 70s of the last century, there was a hope to use sapphire fibres produced by EFG in structural applications so their high temperatures strength was a subject of an intensive study [21, 22, 23, 24]. However, high cost of the fibres produced by crystallisation of the melt has eventually led to losing interest to such fibres as reinforcement in heat-resistant composites technology.

Internal crystallisation method invented by Mileiko and Kazmin was described for the first time about 30 years ago [25, 26]. Since then a main scheme of the method as well as some variation of it has been published in a number of the papers (see references [27, 28, 29, 30, 31,

http://dx.doi.org/10.5772/61024

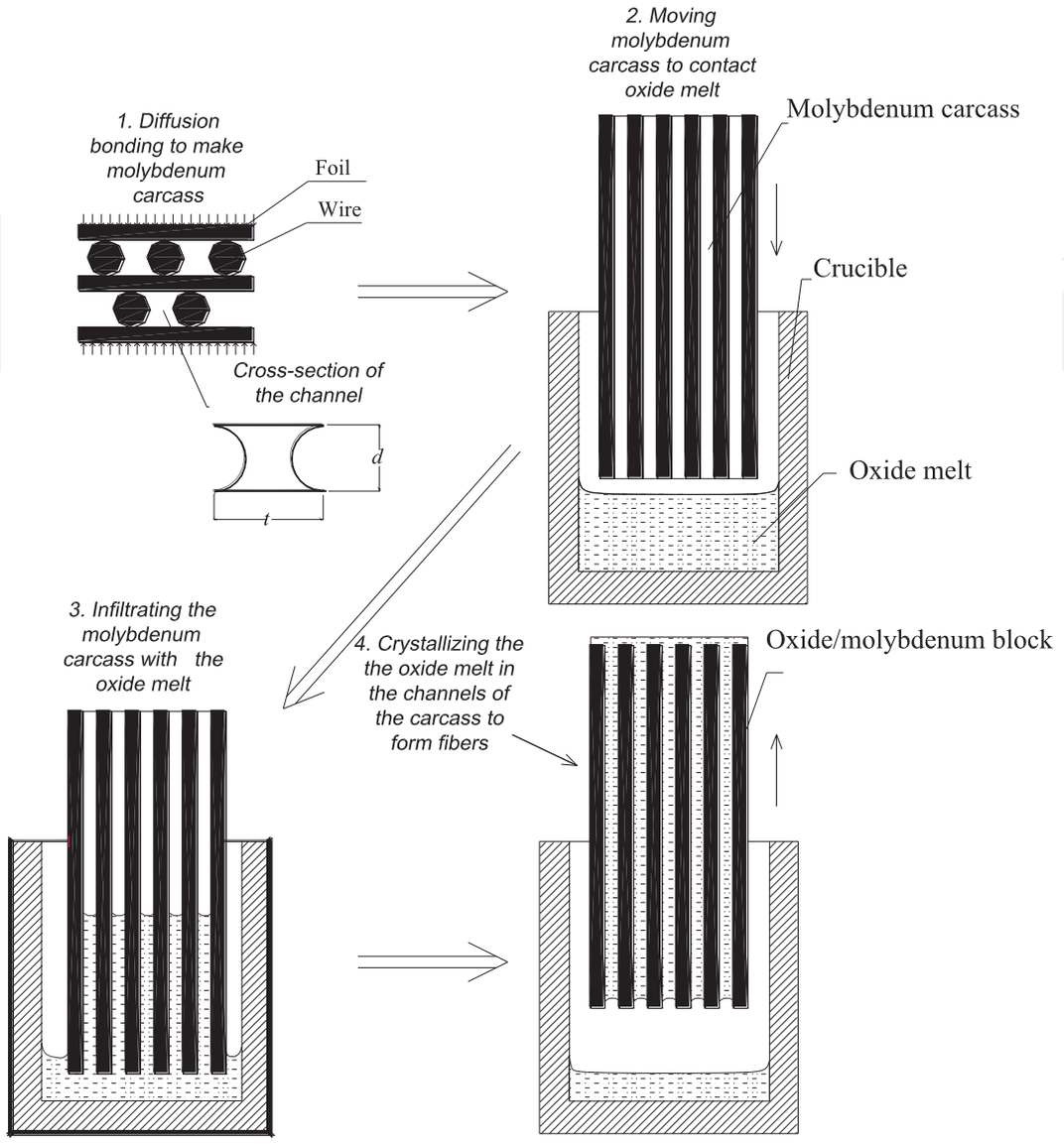

Figure 3. Schematic of the internal crystallization method (ICM).

32, 33]). All these papers are concerned with oxide fibres. However, recently it was shown a possibility to produce a larger family of the fibres. I particular, in Section 7.2 prospects of the internal crystallisation method composites with silicide fibres will be described.

A schematic of the method is presented in Figure 3. A molybdenum carcass with continuous channels in it, which is prepared by diffusion bonding of an assemblage of the wire and foil (step 1 in Figure 3), is infiltrated with an oxide melt (steps 2 and 3) by the capillary force. The melt is then crystallised in the channels to form fibres in an oxide/molybdenum block (step 4). This is a main scheme of the ICM, which can be varied to attain a particular goal. For example, to obtain sapphire fibres of a homogeneaous crystallographic orientation, a seed oriented in an appropiate manner is used as shown in Figure 4.

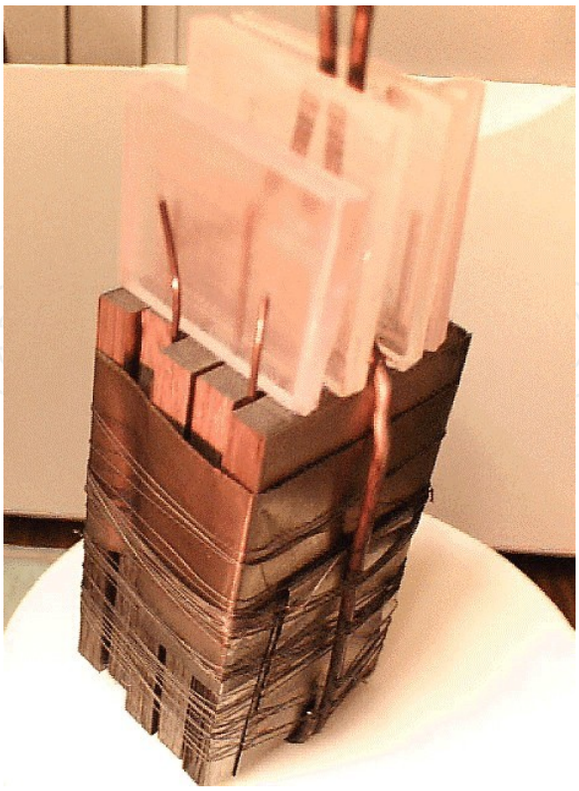

Figure 4. A set of the molybdenum carcass with sapphire seeds at the top of it.

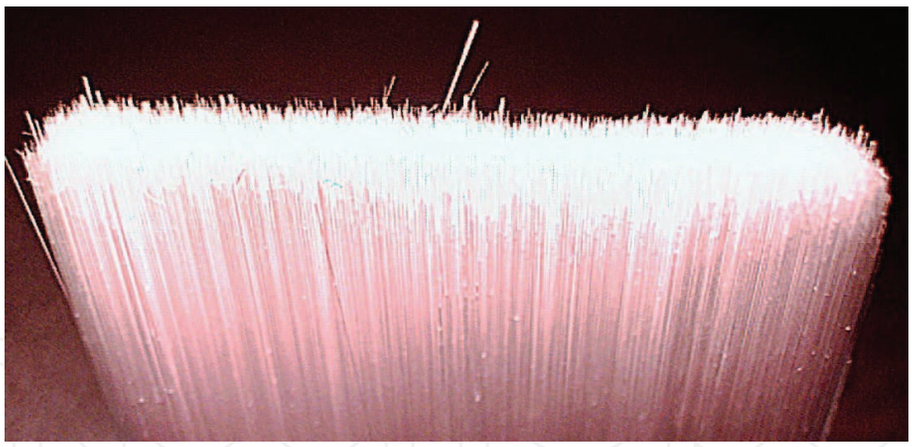

Figure 5. A bundle of sapphire fibres obtained by using ICM.

Finally, molybdenum is dissolved in a mixture of acids to get a bundle of the fibres (Figure 5). At the present time, the length of the fibre bundle can be up to 250 mm. Fibre volume fraction in a molybdenum block is normally about 0.4. The fibre has a cross-sectional shape close to that shown shematically in Figure 3, a characteristic size of it is usually 50 to 300 μm. A number of the blocks, which can be crystallised in one process as shown in Figure 4 is limited only by the size of the thermal zone of the crystallising machine. A set shown in Figure 4 contains after the crystallisation process neary 40,000 fibres with characteristic cross-sectional size of 100 μm.

http://dx.doi.org/10.5772/61024

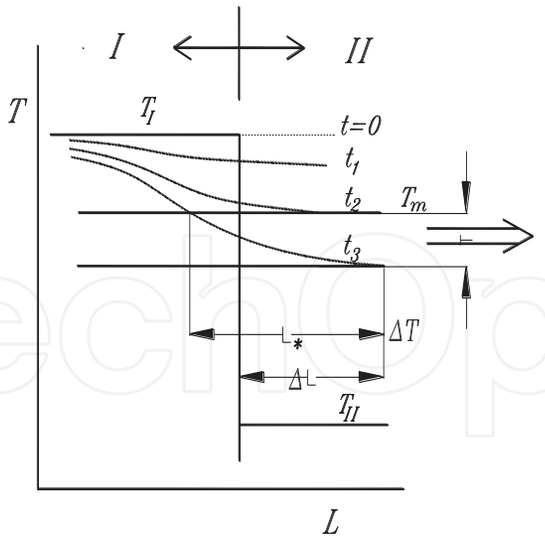

Figure 6. Schematic representation of temperature profiles in the crystallization zone.

3. Structure and mechanical properties of fibres produced by ICM

The microstructure and mechanical properties of fibres produced by ICM are determined mainly by the crystallization process of the fibre in the channels of the auxiliary molybdenum matrix.

3.1. Microstructure of ICM-fibres

A qualitative model of the process is suggested in references [26]. Suppose we have a furnace with two temperature zones "I" and "II" (Figure 6) and there is no direct thermal exchange between them. After the infiltration, the specimen is located within Zone I and its temperature is T_I, which is higher than melting point T_m of the fibre material. Now if the specimen is moved instantaneously in the direction of the arrow by distance ΔL, the temperature profile along the specimen starts changing as shown by lines marked with $t = 0$, t_1, t_2,... When some overcooling, say ΔT, is reached at time t_3, spontaneous crystallization within length L^* occurs. As a result of the process a solid-liquid boundary in each channel is emerged. Then the events can go on in a number of the ways depending on a concrete material.

3.1.1. Sapphire

It is well known that sapphire has no preferable crystallization direction. Hence, if a channel effective diameter is sufficiently small then each crystal on the solid side of the solid-liquid boundary can serve as a seed for further crystallization and the fibres obtained have random crystallographic orientations [26]. It is important to note that the probability of having a single crystal occupying the whole channel transverse section increases with the cross-sectional sizes of the channels decreases. A layer of the fibres in a tensile specimen obtained by using ICM, which illustrates the scheme described is shown in Figure 7.

Figure 7. A layer of the sapphire fibres at the top of a sapphire/molybdenum tensile specimen obtained by ICM.

3.1.2. Yttrium aluminium garnet (YAG)

Fabrication technology of bulk crystal of YAG ($Y_3Al_5O_{12}$) normally includes high temperature annealing of crystals to restore YAG since cooling an overheated melt of the $Y_3Al_5O_{12}$ composition yields decomposition of YAG into alumina and perovskite $YAlO_3$. This stage of the process while obtaining single crystal YAG fibre by using ICM should be avoided because it can cause additional stresses in fibres as recombination of YAG is accompanied by a volume change. Hence, while crystallising garnets by using ICM an overheating of the melts is to be excluded [31, 34].

3.1.3. Mullite

Mullite has been known as most creep resistant oxide [35, 36]. That is why, obtaining single crystal mullite fibres looks as a challenge for the composite community. However, some reasons including a complicated phase diagram of the alumina-silica system [37] set serious problems in crystallising the fibres from the melt while using either EFG or LHPG crystallisation methods.

Using ICM allows crystallising single crystal mullite fibres [34,35, 38]. Crystallisation of a raw melt composed of a mixture of alumina and silica in the channels of a molybdenum block is a more complicated process than that of sapphire. The process was studied in details in references [34,35]. The fibre microstructure is determined by the crystallization process.

To study specific features of crystallisation of the melt containing a mixture of Al_2O_3 and SiO_2, a number of the raw compositions, n Al_2O_3:SiO_2, were used with the value of n = 1.5, 1.8 and

http://dx.doi.org/10.5772/61024

2.05. As in the case of sapphire, the fibre microstructure is changing in the upper portion of the block where crystallisation starts and then remains fairly unchanged. The steady state growth yields the fibres of nearly single-crystalline structure. Typical cross-sections of the fibres corresponding to lowest and highest values of n are presented in Figure 8.

Consider first a fibre obtained from the raw mixtures corresponding to $n = 2.05$ (Figure 8). The X-ray microanalysis shows that the black phase in SEM-pictures has atomic ratio Al:Si slightly higher than that in the precursor ($n = 2.05$). Despite of an excess of alumina in a fibre on the average, in the sharp corners of some fibres a "white" phase can be seen. With the value of n decreasing, an excess of silica in the raw material yields larger areas occupied by the "white" phase (Figure 8a). The "white" phase occurs to be enriched with silica and it is certainly a glassy phase. Again, a composition of the "black" phase corresponds to mullite. Impurities contents in the two phases of the fibres indicate that a growing mullite crystal pushes the impurities, which exist in the melt, to a silica enriched melt that solidifies at a lower temperature to form inclusions of the glassy-phase.

The microphotographs presented and the data of the The X-ray microanalysis [34] reveal some important features of the fibre microstructures:

1. The composition of mullite in the fibres is close to $2Al_2O_3$:SiO_2 independent of the initial composition of the precursor. A rather broad field of the existence of mullite in various phase diagrams published explains deviations from the exact 2:1 molar ratio.

2. Mullite is optically transparent, which is characteristic to single crystal. The content of impurities in the mullite phase does not reach the sensitivity of the experimental method.

3. Inclusions of the glassy phase are located mainly at the fibre periphery.

Optical microscopy [32] shows that the fibers consist of a mosaic of single crystal areas up to about 5 mm in length. The c-axis of the single crystal individuals are misalligned up to ±3° with respect to the fiber axis.

The events occurred in the volume of spontaneous crystallisation in the case of mullite fibres are similar in some details to those while crystallising sapphire fibres and different from it in other details. Observing changes of the microstructure of mullite fibres crystallised from the melts with $n < 2$ along the length of an oxide/molybdenum block provides an insight into the growth mechanisms of mullite that yield a microstructure of the fibre on the steady state growth portion. The microstructure of fibres at the top of an oxide/molybdenum block is presented in Figure 9. One can see a number of the mullite crystals divided by silica-based phase. For example, in an area marked by a circle, three crystals are seen. The direction of all crystals along the fibre axis coincides certainly with c-axis of the mullite crystal. However, their angular orientations can vary.

Crystallisation proceeds with growing some crystals of various angular orientations. The process is accompanied with pushing a liquid, which is to form the glassy phase, towards the oxide/molybdenum interface. Obviously, the crystallisation process depends on many parameters such as pulling rate, temperature gradients, melt composition, etc.

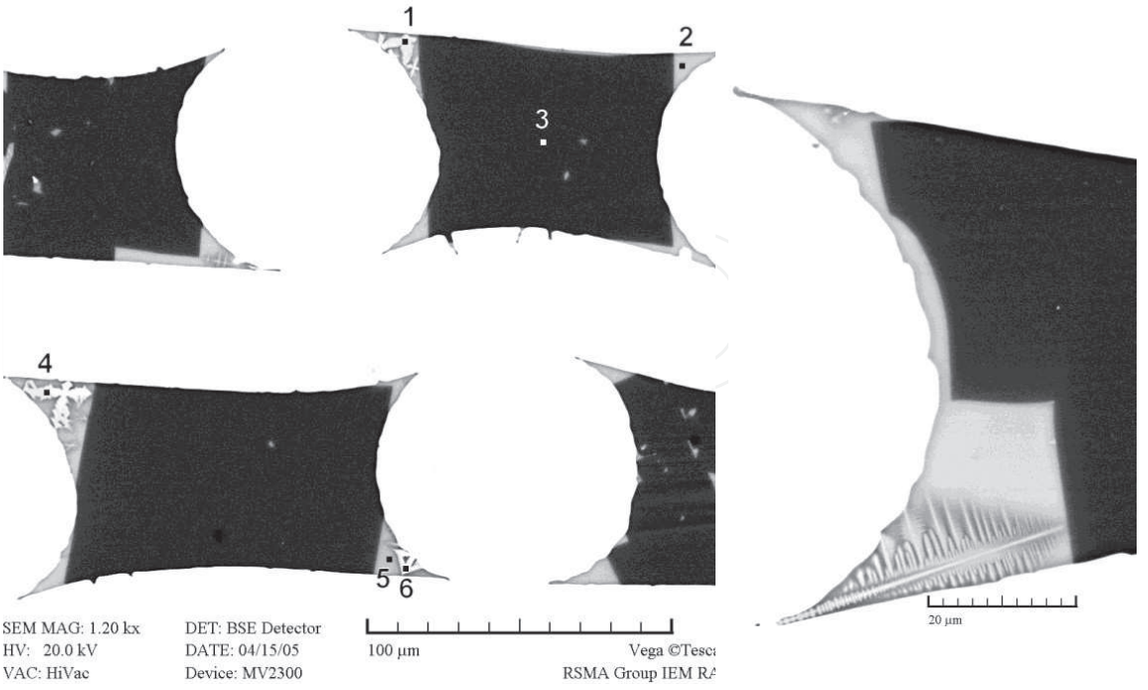

(a)

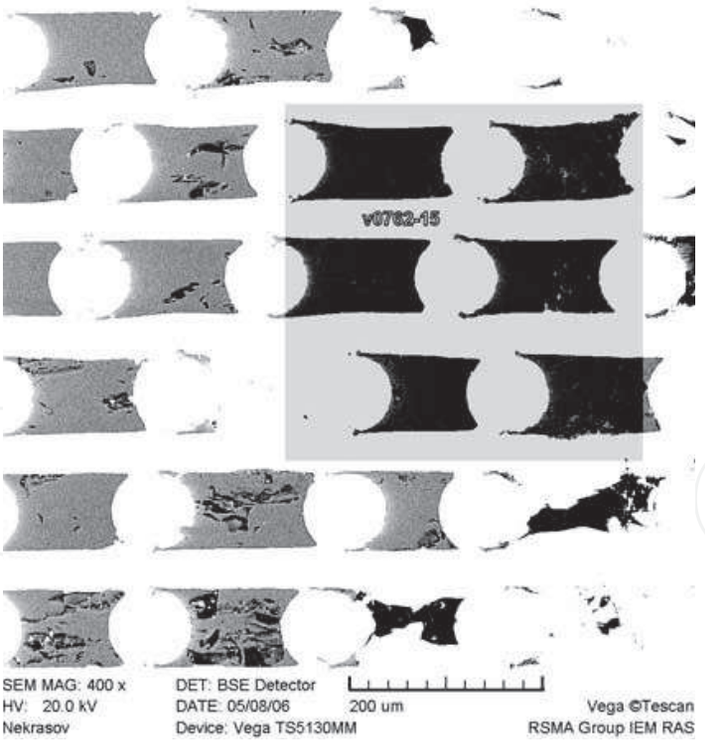

(b)

Figure 8. Typical cross-section of fibres in a region of the steady-state growth obtained from the melt of mixtures $1.5Al_2O_3$:SiO_2.(a) and $2.05Al_2O_3$:SiO_2 (b). Black areas are mullite; white ones are glassy-phase.

http://dx.doi.org/10.5772/61024

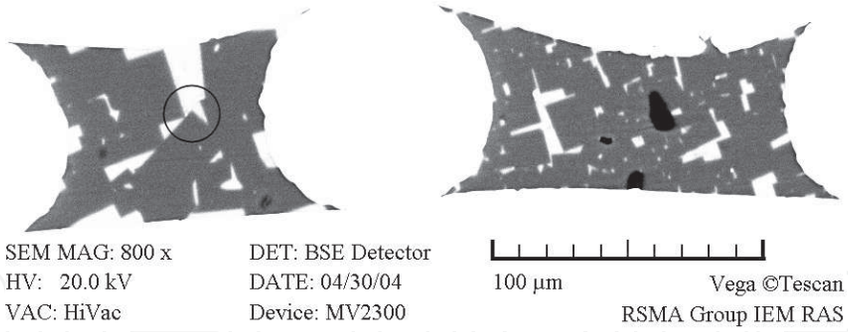

Figure 9. The microstructure of fibres in top of a fibre bundle shown in Figure 8a (raw mixture corresponds mixture $1.5Al_2O_3$:SiO_2).

3.1.4. Oxide eutectics

Special features of crystallization process in the channels of a molybdenum carcass determine particularities of the eutectic microstructure of the fibres. Perhaps, most important feature is a non-plane solid-liquid boundary in the channels due to heat sinks into molybdenum carcass. Still, characteristic microstructure of the eutectics is observed in the fibres obtained by using ICM, Figure 10, 11 and Figure 12 [39]. A non-homogeneity of the microstructures is a result of the features of crystallization process mentioned above. The dependence of the characteristic microstructure size of the Al_2O_3-$Y_3Al_5O_{12}$ eutectic fibres on the pulling rate related to crystallysation rate (Figure 11) is certainly close to a usual one.

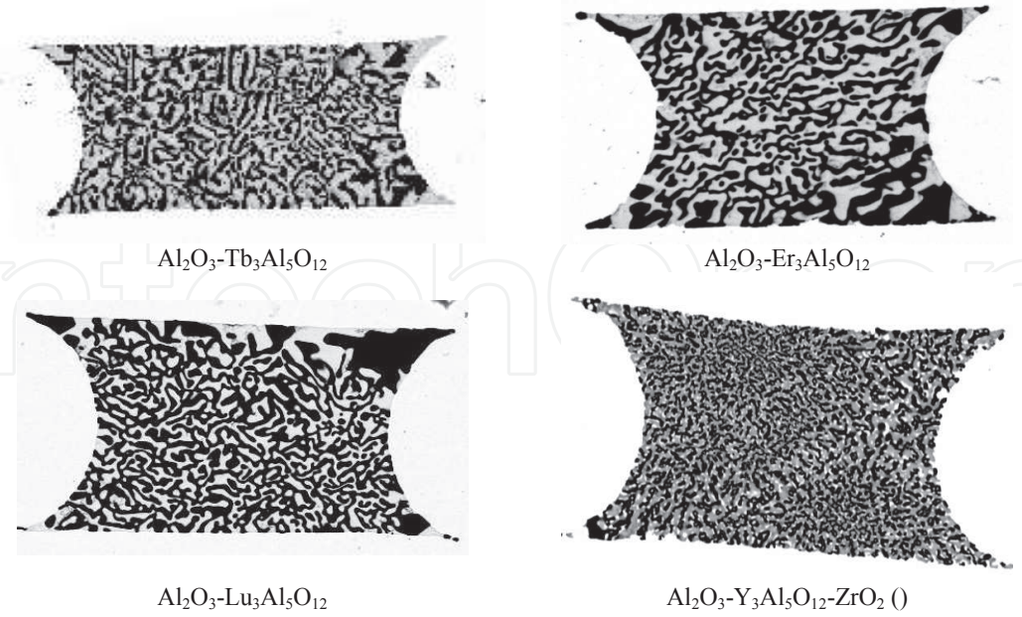

Figure 10. The microstructures of Al_2O_3-$Re_3Al_5O_{12}$ (Re = Tb, Er, Lu) and Al_2O_3-$Y_3Al_5O_{12}$-ZrO_2,eutectic fibres crystallised with pulling rate 1.7 mm/min. Characteristic size of the fibre cross-section (distance between the plane surfaces) is ~65 mm.

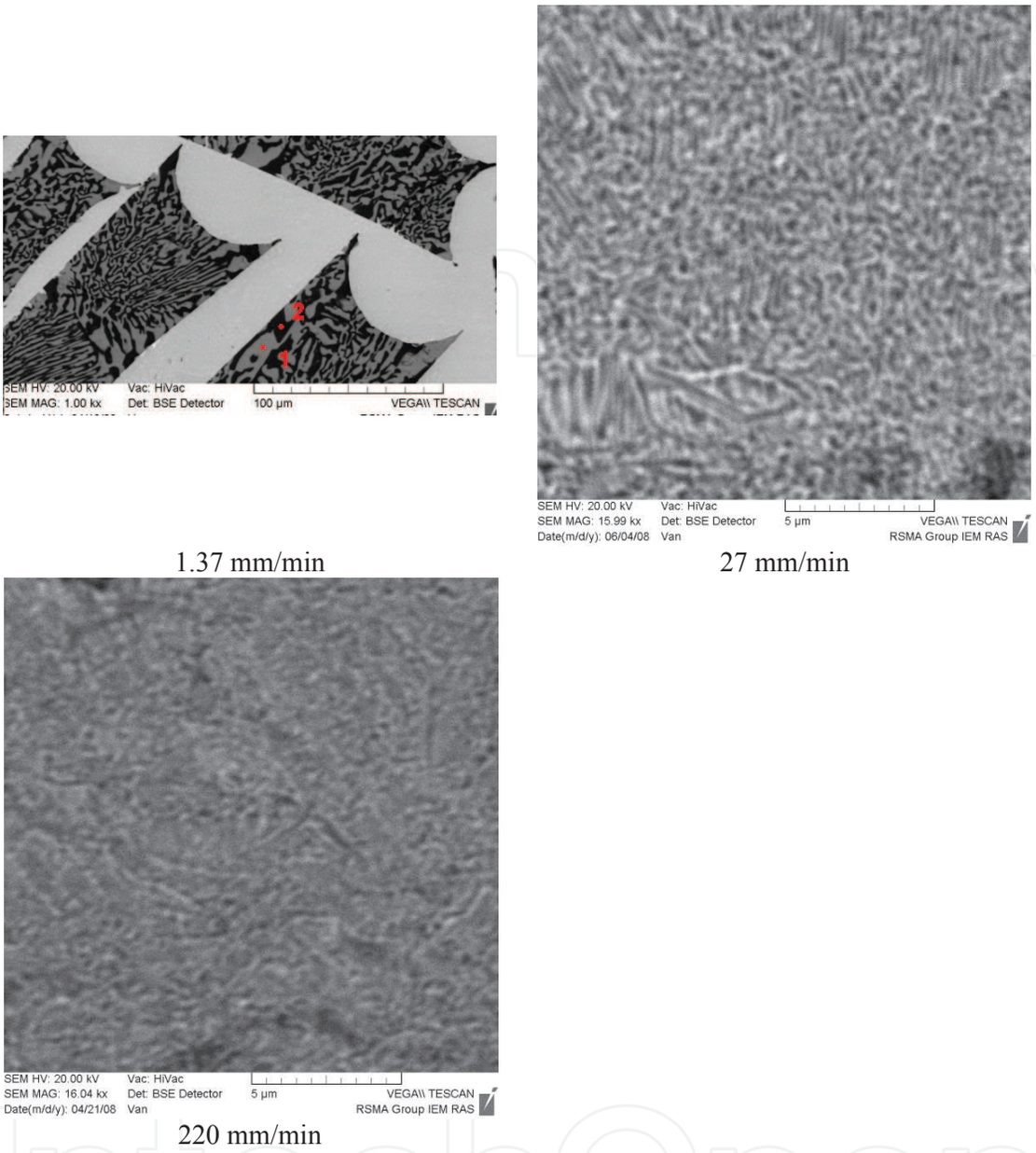

Figure 11. The microstructures of Al_2O_3-$Y_3Al_5O_{12}$ eutectic fibres crystallised with various pulling rate.

3.2. Room temperature strength of fibres produced by ICM

First of all, it should be noted that the strength of fibres produced by using ICM as well as that of all structural fibres depends on their surroundings: the results of testing separate fibres can drastically differ from the effective strength of the fibre in a matrix [40].

Another point to be mentioned concerns methods of measuring strength This is important since the fibres have an unusual shape of the cross-section.

The strength of separate fibres is measured by looping a fibre around a series of the rigid cylinders of successively smaller diameters and calculating the bending strength [41]. The

http://dx.doi.org/10.5772/61024

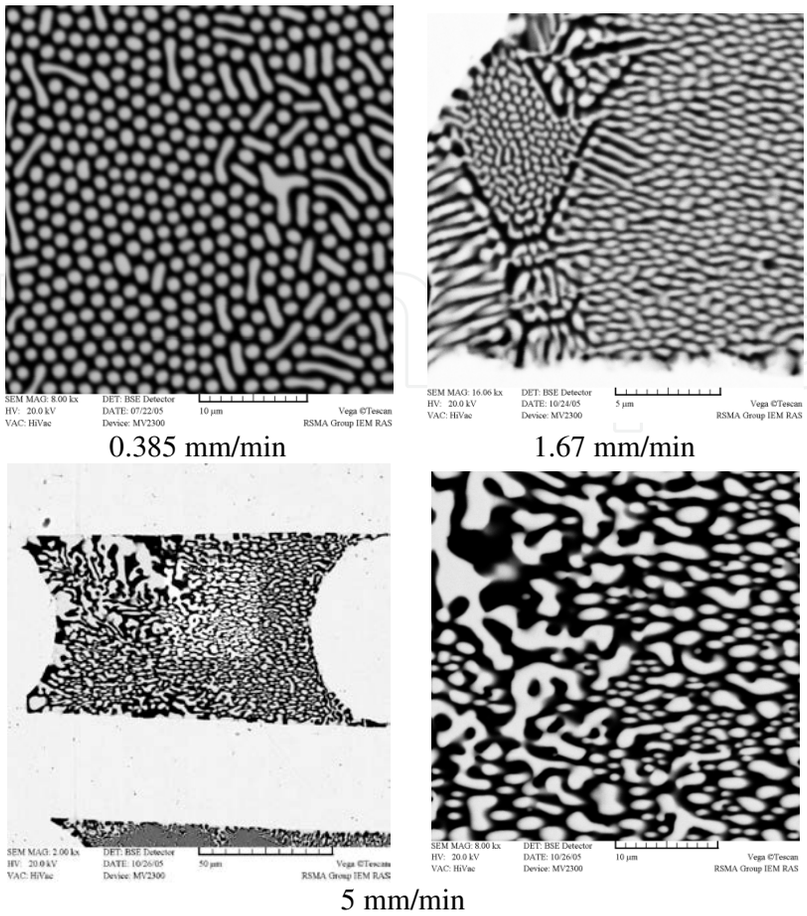

Figure 12. The microstructures of Al_2O_3-$GdAlO_3$ eutectic eutectic fibres crystallised with various pulling rates.

maximum fibre stress corresponding to the rigid cylinder of radius R is calculated according to

$$\sigma = E\frac{d}{2R} \tag{1}$$

where E is the Young's modulus of the fibre material and d is the distance between the plane surfaces of a fibre. To a first approximation, σ is the fibre bending strength at a length equal to the average distance between the fibre breaks.

Results of measuring sapphire fibre bending strength are presented in Figure 13. It should be pointed out that coating the fibre with a thin layer of silicon oxi-carbide by uing CVD process yields an essential increase in the fibre strength. This effect is a result of healing fibre surface defects by the coating material.

An effect of stress concentration in the vicinity of a defect in the fibre can be enhanced as a result of temperature gradients. Hence, annealing fibres in a furnace either without or with small temperature gradients leads to an increase in the fibre strength as shown in Figure 14 and Figure 15 for sapphire and single crystalline YAG fibre, respectively.

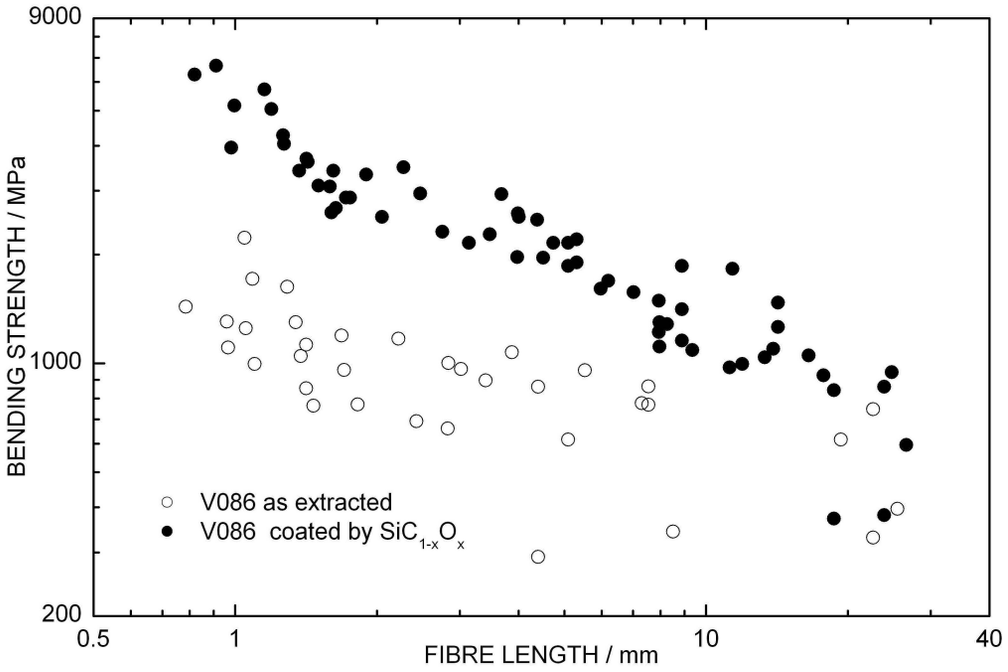

Figure 13. Bending strength of as-extracted and coated sapphire fibres versus fibre length. The fibres are coated by a layer of $SiC_{0.99}O_{0.01}$ of thickness 4-6 μm [33].

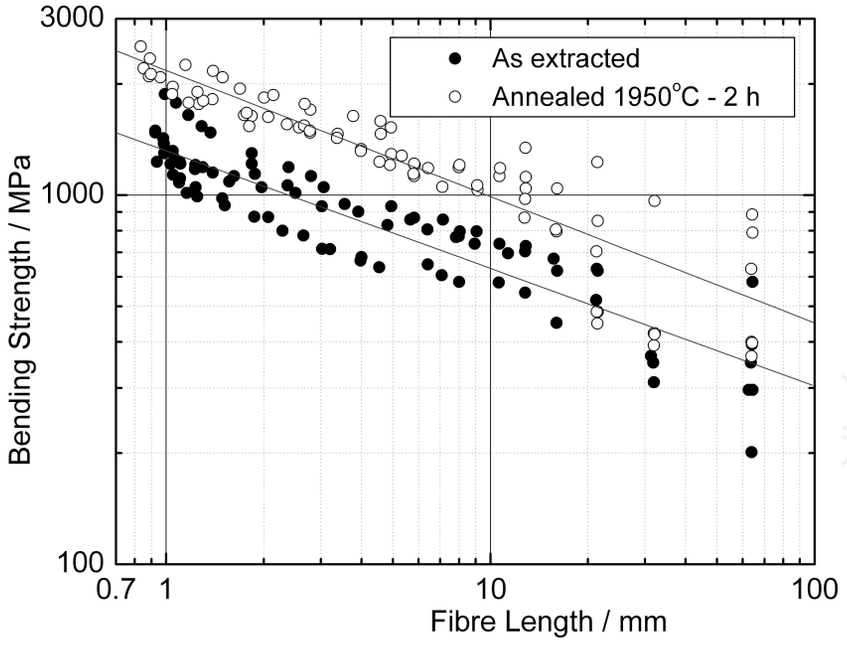

Figure 14. Scale dependence of sapphire fibre strength, as extracted and annealed to decrease permanent stresses. All the fibres are from one batch [33].

The microstructure and strength of eutectic fibre depends on the crystallization rate, with the increasing a characteristic size of the eutectic microstructure is decreasing as shown in Figure

http://dx.doi.org/10.5772/61024

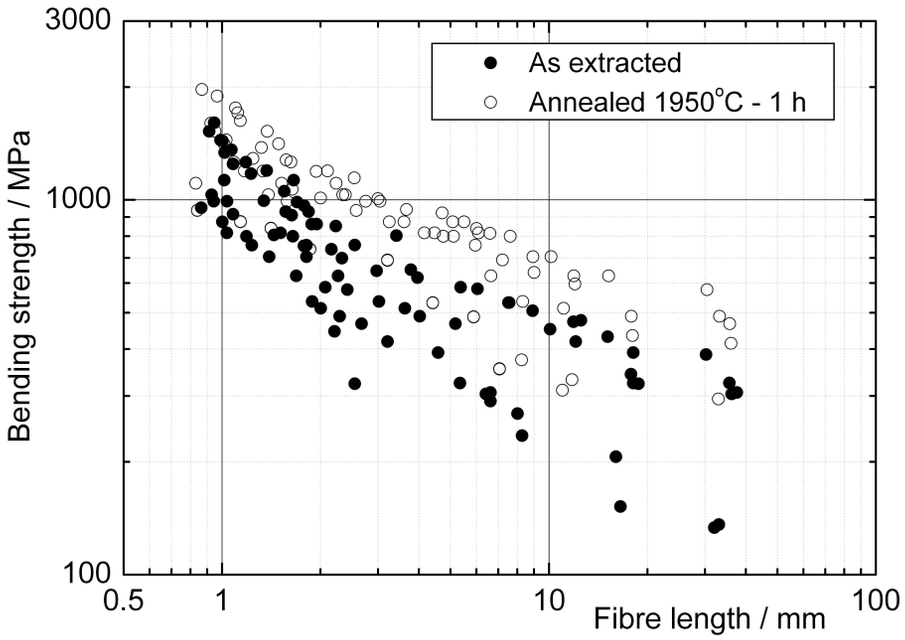

Figure 15. Bending strength versus fibre length for as extracted and annealed YAG fibres. All the fibres are from one batch. [36].

11 and 12. Hence, the strength of eutectics is expected to increase. However, the experiments yield a strength/crystallisation-rate dependence with a maximum at a some value of crystallization rate (Figures 16 and 17). This phenomenon remains to be studied.

3.3. High temperature strength of fibres produced by ICM

The measurements of high temperature strength of ICM-fibres [33] confirm early finding that single crystalline oxides retain their nearly room temperature strength up to high temperatures. Obviously, it is difficult to perform high temperature tests of ICM-fibres in the same manner as it is done at room temperature. However, the method of producing the fibres provides a way to test fibres that is to test oxide/molybdenum specimens. This way has been used from the very beginning of the developing of the internal crystallisation method.

Early experiments with oxide-fibre/molybdenum-matrix composite specimens described in [26,27] were conducted in tension. Then most tests have been performed under bending; such tests can be done with simple specimens. To calculate the fibre strength in molybdenum carcass with volume fraction of the channels of about 40% one needs to know mechanical properties of molybdenum used for the carcass in fully recrystallised state. The necessary data have been obtained in tensile tests, see Figure 18, and the strength/temperature dependence is approximated by a polynom of the 3rd order. The strength data obtained for some fibres are presented in Figure 19 and Figure 20. One can see that (i) the effective strength of ICM-sapphire fibre in the molybdenum matrix does not significantly differ from that for the fibres obtained by EFG method, (i) the fibre strength obtained in bending tests is slightly higher than that obtained in tensile tests, which should be expected.

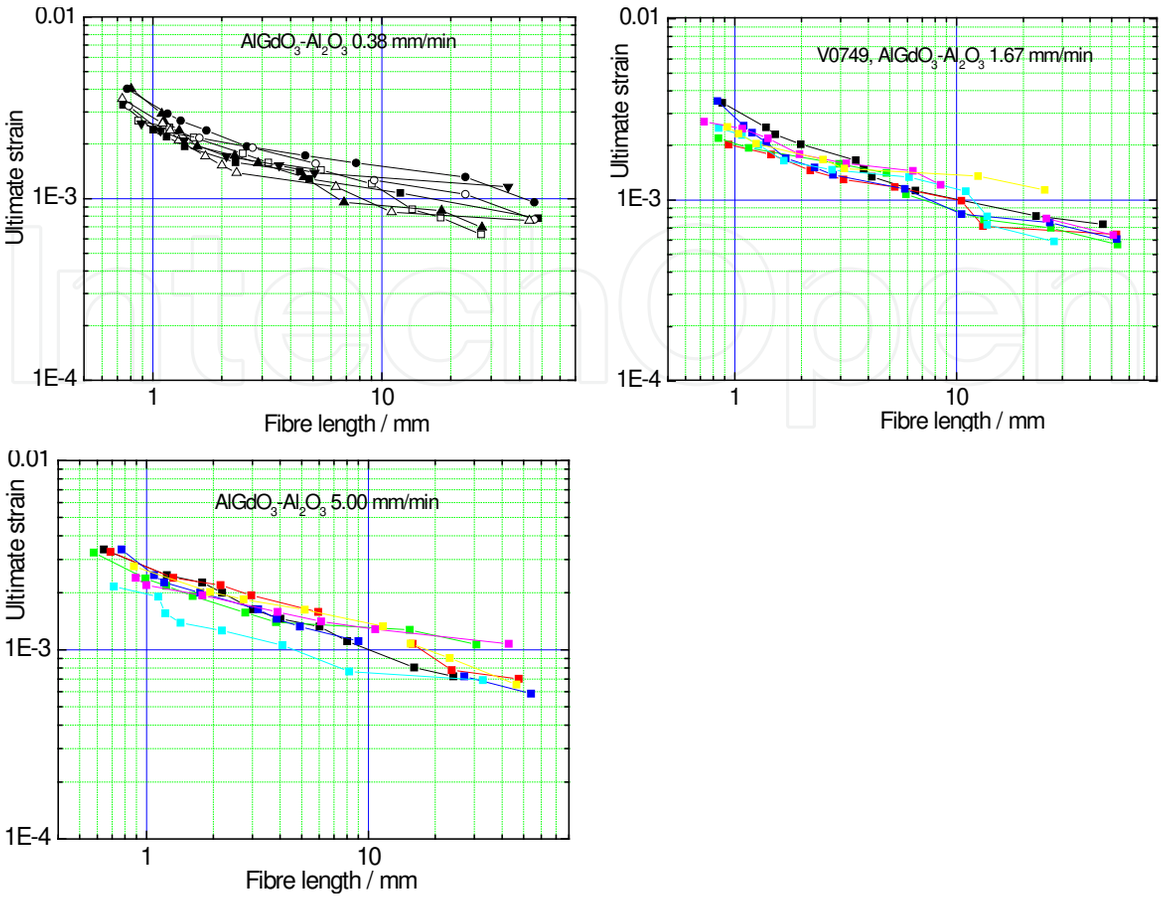

Figure 16. Ultimate strain versus fibre length for Al_2O_3- $GdAlO_3$ eutectic fibres crystallised with various pulling rates.

3.4. Creep characteristics of fibres produced by ICM

Creep characteristics of ICM-fibres are measured by testing oxide-fibre/Mo-matrix composites obtained at step 4 in Figure 3. It should be noted that oxide melts wet molybdenum excellently and the fibres have been crystallised in the channels of the molybdenum matrix, so the fibre/matrix interface is considered to be an ideal; hence, the fibre strength is not affected by possible surface flaws. Therefore, testing fibres in their mother matrix yields their virgin properties. Any further processing of the fibres changes their properties. Note that the fibre characteristics are easily obtainable as a contribution of the matrix, which is fully recrystallised molybdenum, to the creep resistance of oxide/molybdenum composites even at the lowest temperature, 1000°C, is negligible, less than 10 MPa [27].

An analysis of the bending tests performed under a varying load yields approximate creep characteristics of the composite in a particular specimen [42]. This allows excluding a number of the factors, which determine a usual scatter of the creep data of a batch of the material. Performing such tests yields a characterisation of each specimen by its own set of the creep characteristics. The analysis is based on the following assumptions:

1. A composite is characterised by identical creep behaviour under tension and compression

http://dx.doi.org/10.5772/61024

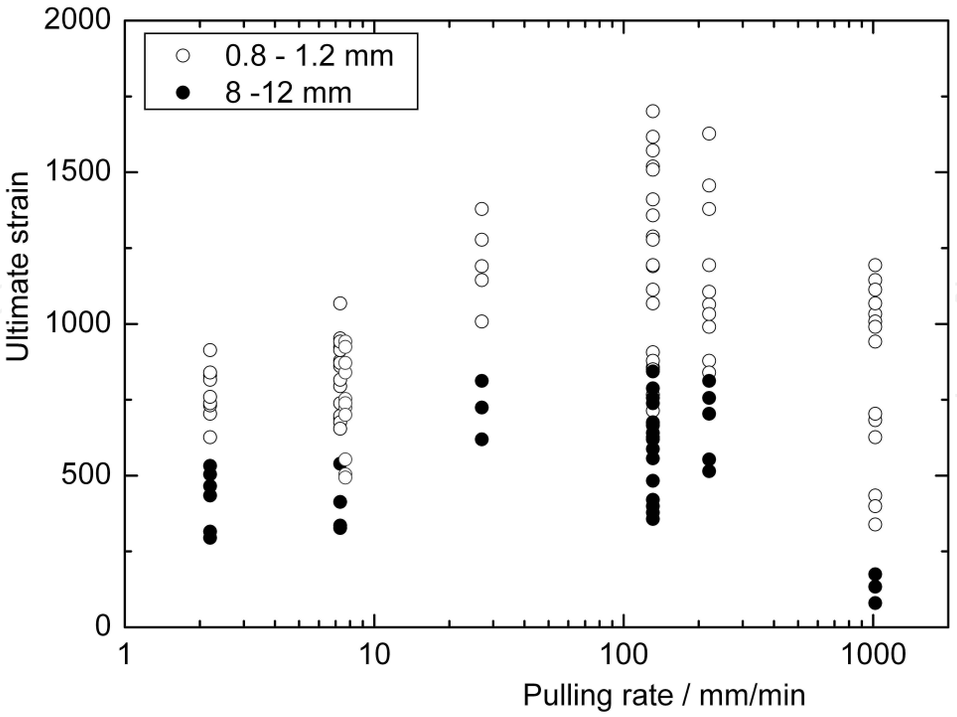

Figure 17. Dependence of the strength of Al_2O_3-$Y_3Al_5O_{12}$ eutectic fibres on two length bases on crystallization rate. The value of the Young's modulus of the eutectic is accepted to be 350 GPa

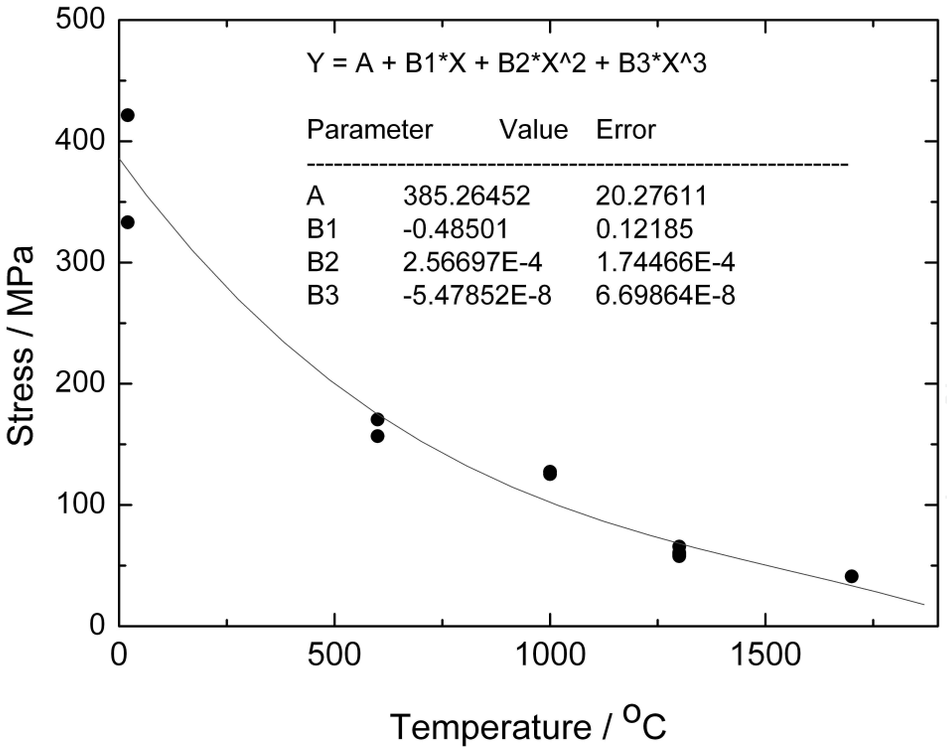

Figure 18. The temperature dependence of the tensile strength of a molybdenum carcass subjected to heat treatment at 2050°C for 30 min [26]. Approximation by a polynom of 3rd order with values of the constants shown.

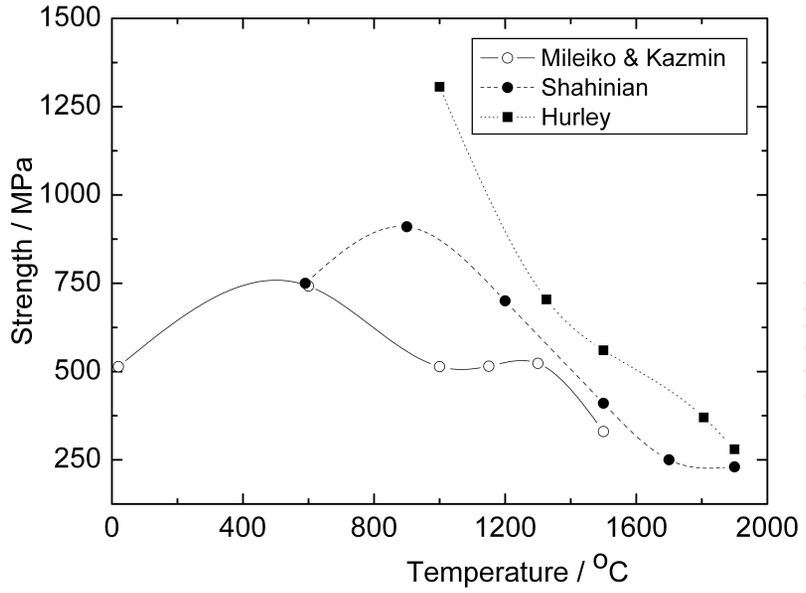

Figure 19. Temperature dependence of the tensile strength of sapphire fibres obtained by both the ICM and EFG-method. Experimental data are after Mileiko and Kazmin [27], Hurley [22] and Shahinian [21]. The present data are obtained by testing sapphire/molybdenum specimens in 3-point bending.

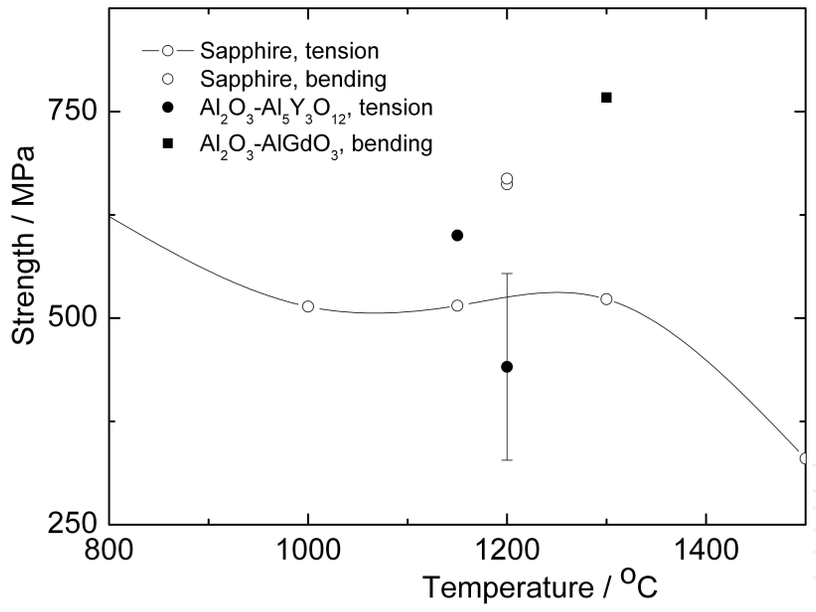

Figure 20. High temperature strength of some oxide fibres produced by ICM. The data were obtained by testing oxide/molybdenum specimens [33].

2. The creep law of the material is

$$\dot{\varepsilon} = \eta_n \left(\frac{\sigma}{\sigma_n} \right)^n \tag{2}$$

http://dx.doi.org/10.5772/61024

where η_n , σ_n , and n are constants. The value of η_n can be chosen arbitrary. In what follows, η_n=10^{-4} h^{-1}, which means that σ_n is the stress to cause 1% creep strain for 100 h. We call this value as creep resistance of a material on 100-hours time base.

A solution of a creep problem for a beam under bending yields a dependence of the deflection rate, $\dot{f}$, of the beam at its centre on applied load Q [43]. For a beam of rectangular cross-section of height $2h$ and width b we have:

$$\dot{f} = \eta_n \frac{1}{2^{3n+2} n^n (n+2)} \left(\frac{Q}{\sigma_n h^2} \right)^n \left(\frac{L}{b} \right)^n \left(\frac{L}{h} \right) L \tag{3}$$

for 3-point bending. The solution was obtained neglecting a contribution of shear deformations to the displacement.

Therefore, measuring $\dot{f}(Q)$ yields the value of exponent n directly and then applying Eq. (3) gives the value of σ_n .

The results of testing some fibres are presented in Figure 21, Figure 22 and Figure 23. In these Figures corresponding data for bulk single crystals are also plotted.

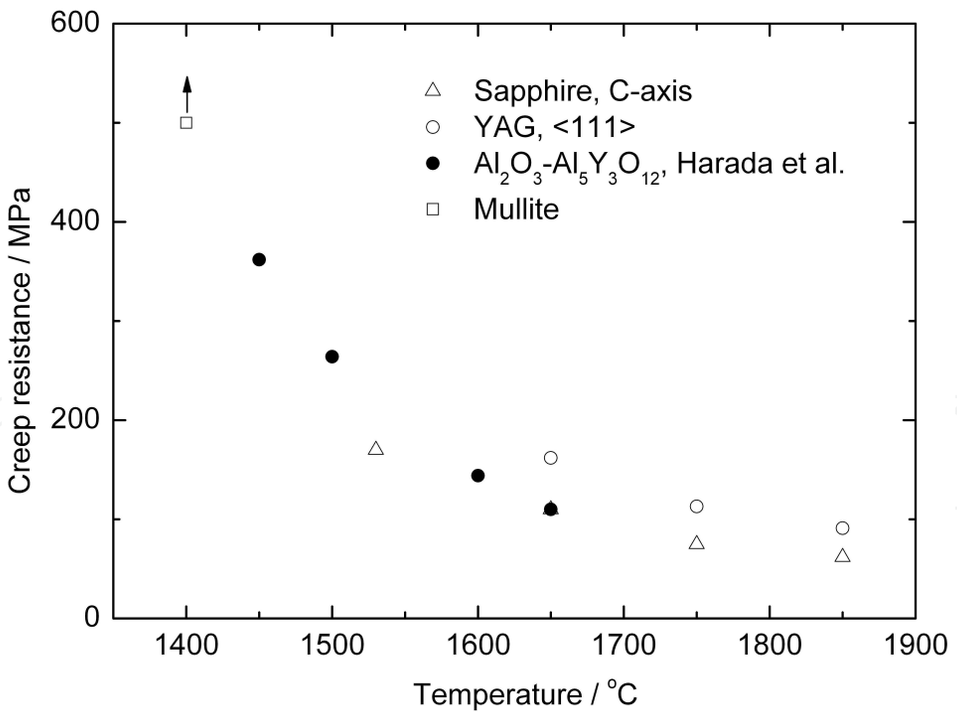

Figure 21. Temperature dependence of the creep resistance (a stress to cause 1% creep strain for 100 h) of some oxides in the form of bulk crystals. Data on sapphire and garnet YAG are after Corman [44], on mullite are after Dokko et al. [35], on Al_2O_3-$Al_5Y_3O_{12}$-eutectics are after Harada et al. [45].

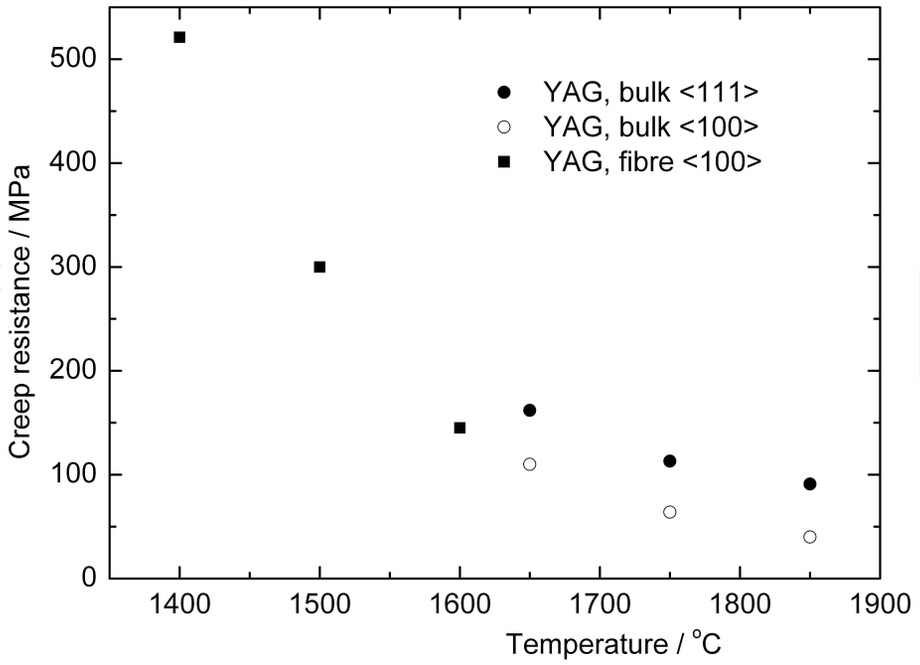

Figure 22. Creep resistance (stress to cause 1% creep strain for 100 h) of bulk YAG crystals of two orientations obtained by using experimental data by Corman [46] and ICM-fibres of YAG obtained by testing oxide/molybdenum specimens loaded in 3-point bending.

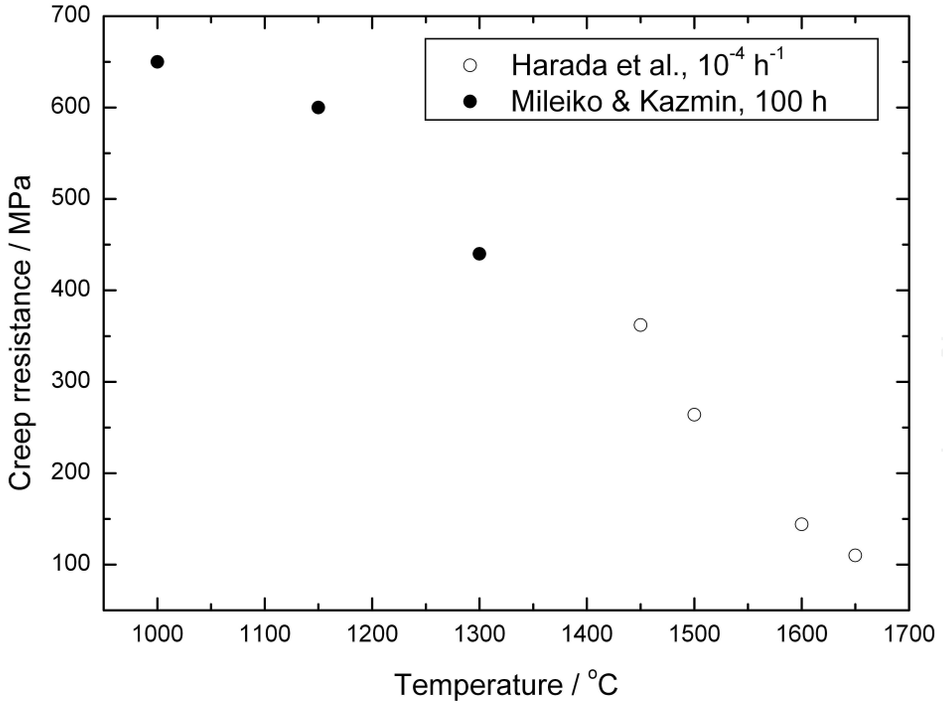

Figure 23. Creep resistance of bulk crystals of alumina-YAG eutectic obtained by using experimental data by Harada et al. [48] and creep rupture stress on the base of 100 h of alumina-YAG eutectic ICM-fibres obtained by using experimental data by Mileiko and Kazmin [46] on tensile creep rupture tests of molybdenum-matrix composites.

http://dx.doi.org/10.5772/61024

Comparing creep resistance of ICM-fibres and bulk crystals for yttrium-aluminium garnet shows an excellent correspondence of creep resistance of bulk crystals and corresponding fibres grown from melt. The data presented provide also an additional confirmation of the validity of the method of evaluation of creep properties of ICM-fibres by testing in bending oxide/molybdenum specimens. Creep resistance of Nextel 720 fibre (α-Al_2O_3+mullite) evaluated from experimental data presented in [50] is also shown in Figure 24. A number of important conclusions can be drawn, in particular:

1. In temperature interval from 1100 to 1600°C, values of the creep resistance of single crystalline YAG and mullite as well as that of alumina-YAG-eutectic fibres obtained by using ICM are nearly the same. YAG fibre looks slightly better than the others. Still, their creep resistance can be certainly enhanced by crystallising them in the <111> direction.

2. Single crystalline mullite fibre produced by ICM does not seem to be superior to, say, YAG fibres. Its creep resistance differs essentially from the experimental point by Dokko et al.

3. Polycrystalline oxide fibres obviously lose their creep resistance below a temperature of 1200°C certainly due to an intrinsic behaviour of grain boundaries (see Figure 24).

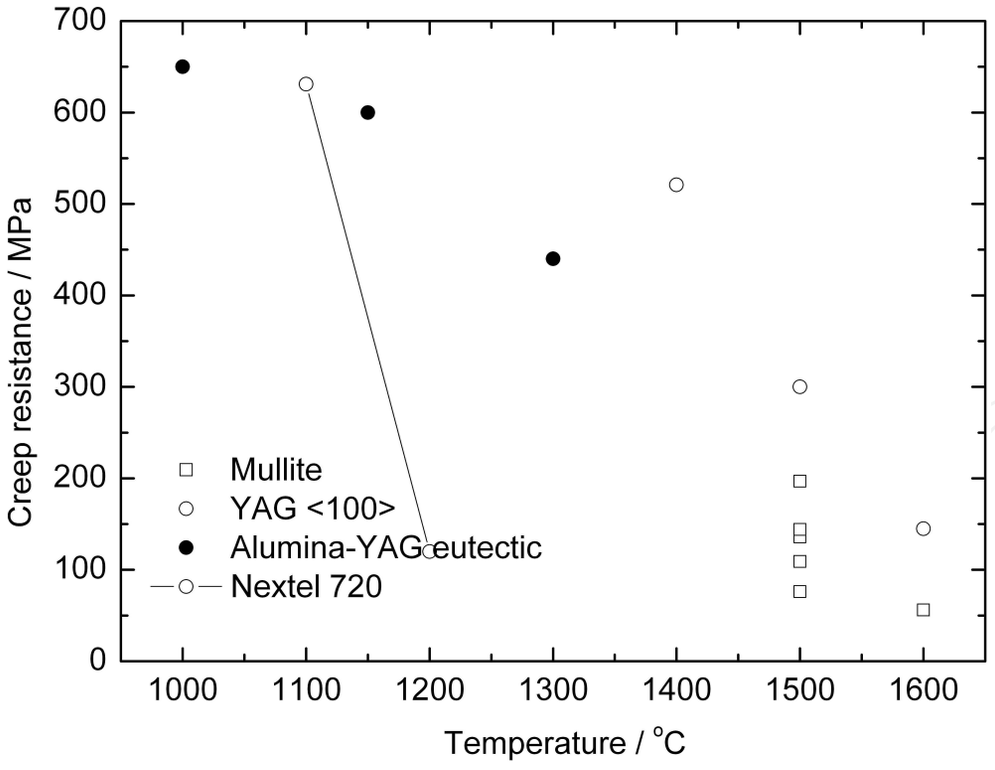

Figure 24. Creep resistance (stress to cause 1% creep strain for 100 h) of ICM-fibres in comparison with commercially available polycrystalline oxide fibres [47].

4. Nickel-based composites reinforced with ICM-fibres

4.1. Preliminary notes

First of all, it should be noted that there are three most important characteristics of heat resistant composites, those being creep resistance, fracture toughness and oxidation resistance. In the case of nickel alloys as matrices for oxide fibres composites sufficiently high oxidation resistance and fracture toughness are to be expected. That is why we will focus here on creep behaviour of nickel-based composites reinforced with ICM-fibres.

On a fundamental study stage of developing composites the main bulk of creep tests are conducted by bending simple composite specimens and then calculating tensile creep characteristics of the composites according to the method developed in [42]. The dependence of displacement rate $\dot{f}$ of the specimen on load Q for a specimen with a circular cross-section of radius R is similar to Eq.(3):

$$\dot{f} = \eta_n \frac{L}{2^{2(n+1)}\left(n+2\right)\mu\left(n\right)}\left(\frac{Q}{\sigma_n R^2}\right)^n \left(\frac{L}{R}\right)^{n+1} \tag{4}$$

where $\mu(n)$ is expressed via gamma-function $\Gamma(\bullet)$:

$$\mu\left(n\right) = \frac{2^{2+\frac{1}{n}}}{3+\frac{1}{n}} \frac{\left(\Gamma\left(1+\frac{1}{2n}\right)\right)^2}{\Gamma\left(2+\frac{1}{n}\right)}.$$

All other symbols are as in Eq. (3).

Such an approach to the creep tests simplifies and speeding up the procedure. The experiments can be even more speeded up if the microstructural creep model developed in reference [51] is used in the analysis of experimental data [48].

The model mentioned yields a dependence of composite stress σ on steady state creep rate $\dot{\varepsilon}$

$$\sigma = \lambda\sigma_m \left[\left(\frac{\sigma_o^{(f)}}{\lambda\sigma_m}\right)^{\beta}\left(\frac{l_o}{d}\right)\right]^{\frac{m+1}{n}} \left(\frac{\dot{\varepsilon}}{\eta_m}\right)^{\frac{1}{n}} V_f + \sigma_m \left(\frac{\dot{\varepsilon}}{\eta_m}\right)^{\frac{1}{m}} V_m \tag{5}$$

where fibre characteristics are determined by the Weibull based strength/fibre length dependence, $\sigma_*^{(f)}(l) = \sigma_o^{(f)}(l_o)\left(\frac{l}{l_o}\right)^{-\frac{1}{\beta}}$; matrix characteristics are given by the power low of matrix creep,

http://dx.doi.org/10.5772/61024

$\sigma = \sigma_m \left(\frac{\dot{\varepsilon}}{\eta_m} \right)^{\frac{1}{m}}$; $n = m + \beta + m\beta$, d is a characteristic fibre diameter; λ is a function of fibre/matrix interface strength α, $0 < \alpha \leq 1$, α = 1 correspond to the ideal interface, which means that its strength is equal to the matrix strength.

Let us approximate Eq. (5) by a power function normally accepted while interpreting experimental data on creep of any materials. An important point is a possibility to calculate the value of exponent q in the approximation

$$\sigma = C\dot{\varepsilon}^{1/q} \tag{6}$$

Rewriting Eq. (5) as

$$\sigma = AV_f \dot{\varepsilon}^{1/n} + B(1 - V_m)\dot{\varepsilon}^{1/m} \tag{7}$$

and searching for values of q and C to provide the best approximation of Eq. (7) by Eq. (6), which means to find a minimum to the integral

$$\Sigma = \int_{\dot{\varepsilon}_1}^{\dot{\varepsilon}_2} \left(AV_f x^{1/n} + B(1 - V_m)x^{1/m} - Cx^{1/q} \right)^2 \mathrm{d}x \,, \tag{8}$$

in which the integration limits are an interval of creep rates of interest. In the present context they are normally 10^{-4} and 10^{-1} h^{-1}.

A comparison of exponent q calculated and the exponent values obtained in the experiments with 2-steps loading of specimens is presented in Figure 25. One can see, that the calculations yield an acceptable result.

Note that a developing of oxide-fiber/nickel-based matrix composites has been meeting a number of the problems. The first one that is finding appropriate oxide fibres has been solved by inventing ICM.

The authors affiliated to NASA described what seemed to be the second problem. They found that sapphire fibres degraded during a liquid infiltration fabrication process. This was observed in testing fibres extracted from the matrix [49]. They concluded that the sapphire fibre is not an appropriate reinforcement for nickel alloys. The experiment was correct, but the conclusion was not completely correct. It will be shown below that the matrix melt interacts with the fibre and causes the fibre degradation but after melt crystallised the matrix heals the defect resulting from the interaction provided there is a good adhesion between the fibre and matrix. Moreover, preexisting defects can also be healed [42, 50]. In fact, the conclusion mentioned can be a kind of the delusion. The real problem is to find ways to organize a strong interface between an oxide fibre and nickel-based matrix.

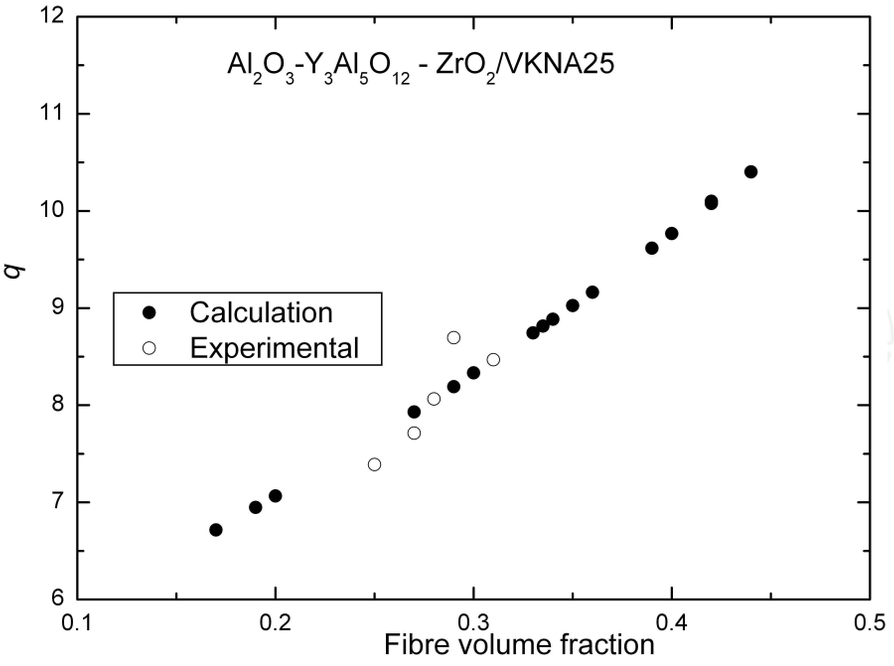

Figure 25. Calculated values of the exponent, q, and the values obtained in the experiments. The values of structural parameters of the composite are: m = 5, β = 3, l_0=1 mm, d = 0.1 mm, α = 0.4, which corresponds to the effective fibre strength equal to 600 MPa [44]. The test temperature is 1150°C.

4.2. Fabrication of nickel-based composites reinforced with ICM-fibres

Three commercially available Russian superalloys have being used as matrix materials. The alloy marked as VKNA-4U contains Al, Cr, W, Ti, Co, Mo and C. That marked as VKNA-25 differs from VKNA-4U by the presence of 3.5% rhenium. The GS-32 alloy contains Al, Cr, Mo, W, Ta, Co, Nb, Re, C, B.

Since Ni-based alloys do not normally wet oxides, pressure casting is used to produce the composites. To fabricate specimens for mechanical testing, a special simple mould was designed that is composed of external quartz tube with one end closed, internal alumina tube with open ends, porous alumina plug at the top of the fibre bundle, and alumina bed at the bottom of the quartz tube [51]. Temperature and pressure of argon gas in the infiltration process were 1550°C and 5 atm, respectively. Crystallisation of the matrix was performed in the axial temperature gradient to make either a single crystalline or columnar microstructure of the matrix. The diameter and length of the specimens were ~5 and ~50 mm, respectively.

4.3. Mechanical properties of nickel-based composites reinforced with ICM-fibres

Creep experiments were carried in 3-point bending by either step-wise loading and in such case the value of the exponent in a creep power law is determined directly or by a single load, in which case the exponent is calculated as shown above. Then tensile creep characteristics of the composites are calculated according to a procedure also described above. Some examples of dependencies of the creep resistance (accepted as a stress to cause 1% creep strain for 100 h) on fibre volume fraction are presented in Figure 26.

http://dx.doi.org/10.5772/61024

It can be seen that for a particular composite creep resistance can reach a value of 150 MPa at a temperature of 1150°C. It is important to note that the density of the composites under consideration is between 6.5 and 6.8 g/cm^3; the density of modern superalloys are approaching 9 g/cm^3.

A compilation of the data presented in Figure 26 is plotted in Figure 27 as a correlation of the maxima of creep resistance of the composites reinforced with various oxide fibres on fibre volume fraction. Such presentation that shows by arrows the possible developments demonstrates clearly an effect of particular fibre/matrix combinations on the creep properties of the oxide-fibre/nickel-based-matrix composites.

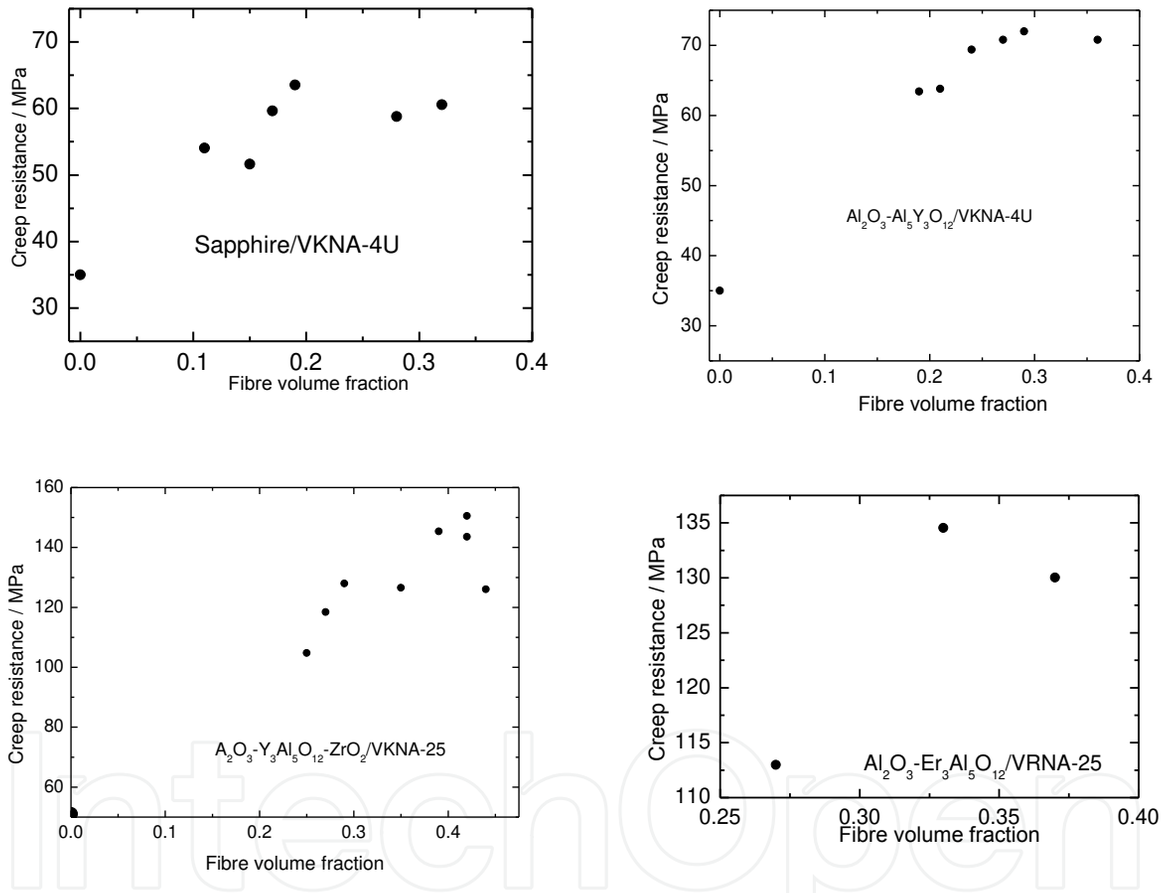

Figure 26. Creep resistance of oxide-fibre/Ni-based-alloy matrix composites versus fibre volume fraction at 1150°C.

Load/displacement curves for AYZ/VKNA-25-matrix composites tested in 3-poit bending at room temperature presented in Figure 28 illustrate two important peculiarities of strength and deformation behaviour of MMCs worth to be mentioned in the present context. First, the curves reveal non-brittle behaviour of the composites even when volume fraction of the brittle constituent reaches 0.48. Such behaviour is to be related to a special fracture toughness properties of MMCs referred to in the Introduction. Secondly, a sequence of the curves for 0 – 0.15 – 0.18 – 0.48 fibre volume fractions reflects another feature of the strength behaviour of

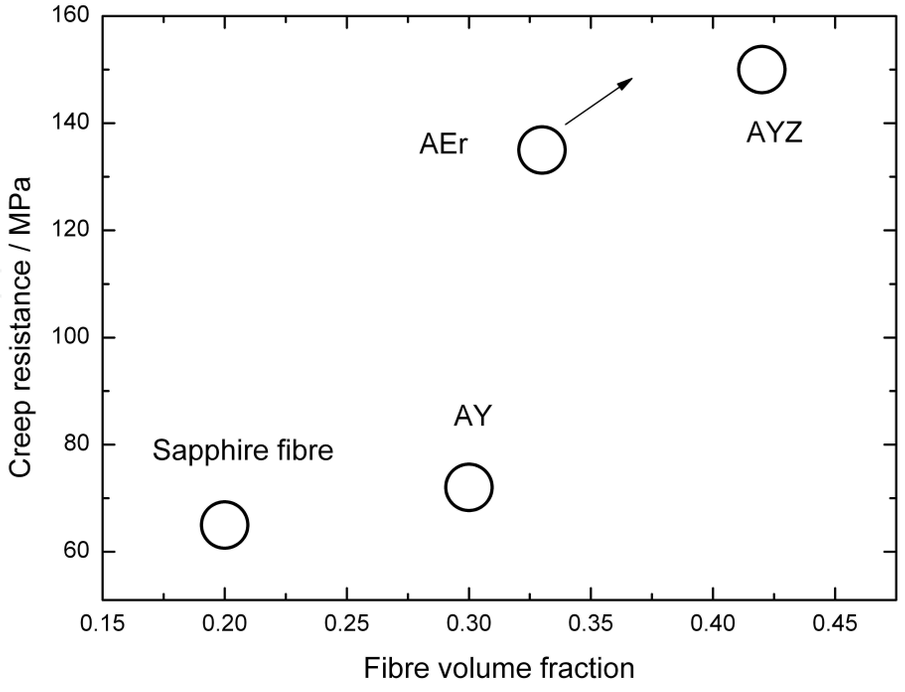

Figure 27. Maxima of the creep resistance of various composites.

MMCs that is the existence of a maximum on a dependence of the strength on fibre volume fraction. This remark is important for a discussion of strength/temperature dependence for an oxide-fibre/high-entropy-matrix composite below, in Section 5.

5. Composites with a high entropy metal matrix

An invention of high entropy alloys (HEAs), which are normally composed of five or more elements each with concentration between 5–35 atomic percent [53, 54] stimulated the opening of a new chapter in the high-temperature metal matrix composites because (i) among such alloys there are some with both high melting points and sufficiently high oxidation resistance [55] and (ii) equiatomic compositions of HEAs promises an easier solution of the wetting problem while dealing with oxide reinforcements. Hence, the author's research group together with a Ukrainian group performed the first experiments aiming at the understanding of prospects of oxide-fibre/HEA-matrix composites [56].

Fibres of Al_2O_3-$Al_5Y_3O_{12}$ and Al_2O_3-$Al_5Y_3O_{12}$-ZrO_2 eutectics were used as reinforcements. A high entropy alloy containing Fe, Co, Ni, Cr and W with a melting point of about 1450°C was chosen as the matrix. The alloy is composed of two phases, those being a base BCC phase and inclusions of a μ-phase of the Fe_7W_6-structure containing all the elements of the alloy, but with their ratios differing from that of the base phase [57].

Specimens were again produced by pressure liquid infiltration of a fibre bundle located in quartz casting mould with the matrix melt. In these experiments, a molybdenum foil 25

http://dx.doi.org/10.5772/61024

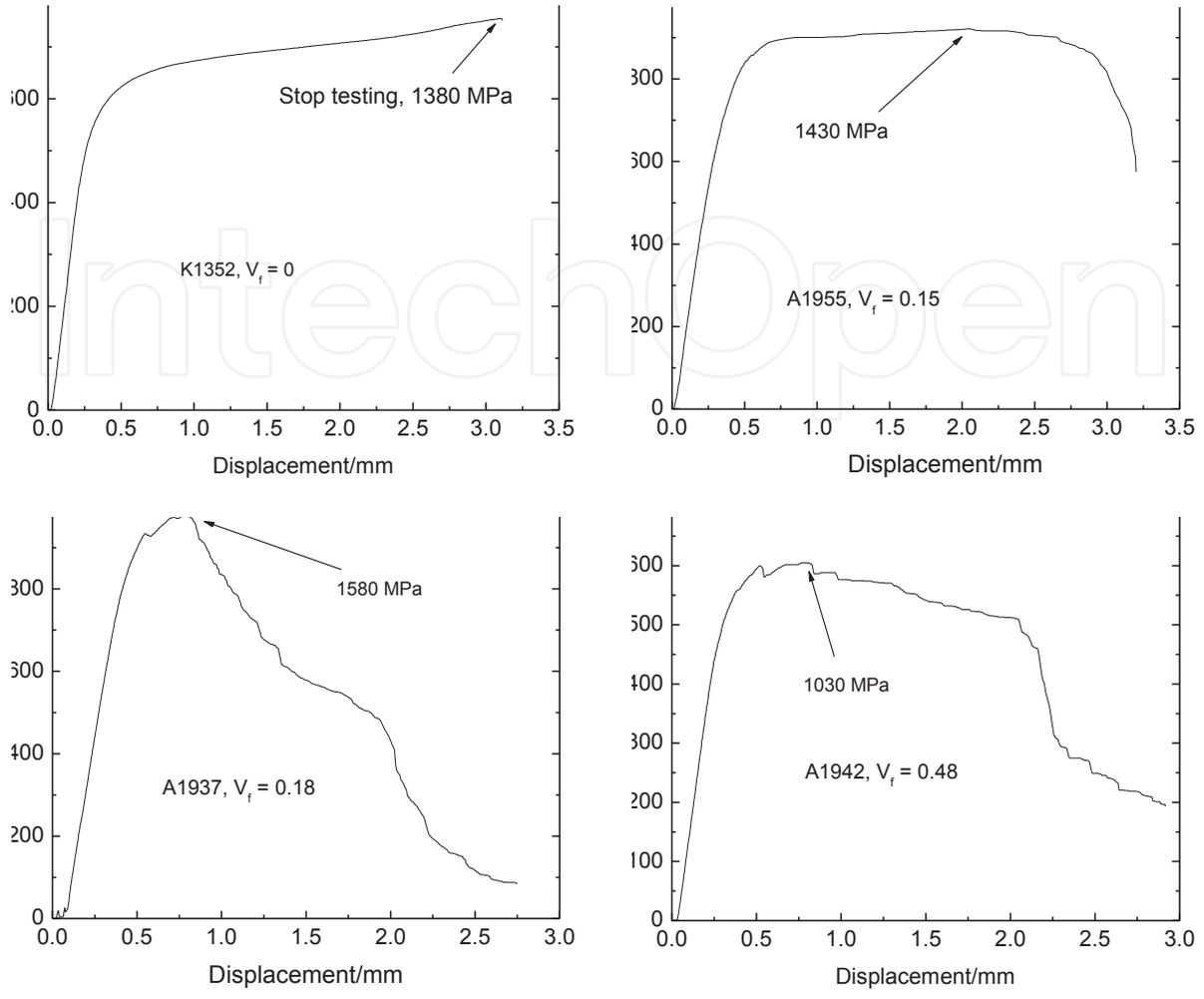

Figure 28. Load/displacement curves for AYZ/VKNA-25-matrix composites tested in 3-poit bending at room temperature [52].

microns thick covered the inside surface of the mould to prevent the interaction between the HEA melt and silica. The necessary gas pressure in this case, 1 – 1.5 atm., is much lower than that in the case of infiltrating oxide fibres with nickel superalloys, which is no less than 5 atm. This is indicative of good wetting in this system, which determines a sufficiently high strength of the fibre/matrix interface.

The microstructure of the composite is illustrated in Figure 29. The results of The X-ray microanalysis of the matrix shows that the base phase (grey phase in the Figure) contains all the elements in nearly equi-atomic ratios, tungsten being an exception. The composition of an inclusion (white phase) is close to $Fe_{1-(x+y+z)}Cr_xCo_yNi_zW_6$. In these experiments, all specimens have relatively large fibre volume fractions, between 40 and 50%.

Composite specimens were tested in the 3-point bending to measure the strength at 20 - 1300°C. Temperature dependence of the strength is presented in Figure 30. The experiments yields two interesting observations.

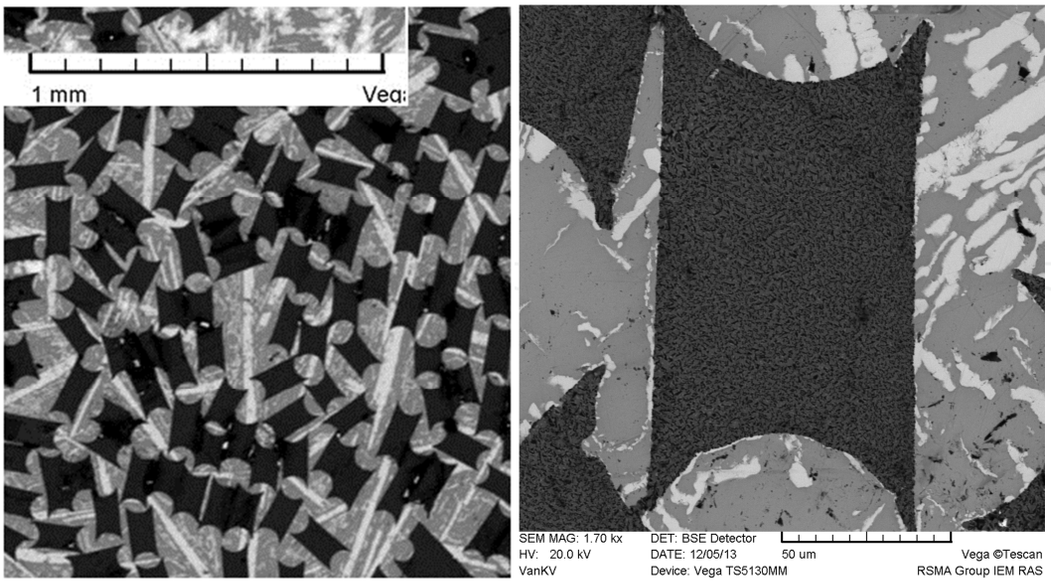

Figure 29. (a) A micrograph of a part of the cross-section of a specimen with Al_2O_3-$Y_3Al_5O_{12}$-eutectic fibre. (b) The microstructure at higher magnification.

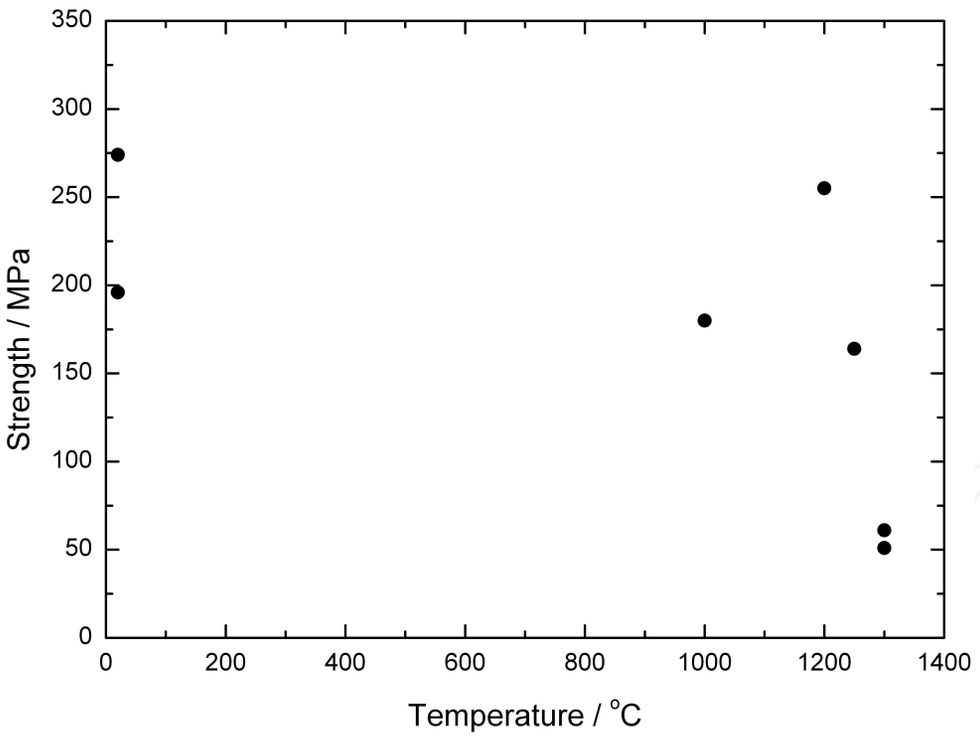

Figure 30. Temperature dependence of the bending strength of the composites reinforced with Al_2O_3-$Y_3Al_5O_{12}$-ZrO_2-eutectic fibre. The fibre volume fractions are between 40 and 50%.

First, the room temperature strength values are relatively low and this is to be the case since the specimens have large fibre volume fractions. The dependence of strength of a brittle-fibre/

http://dx.doi.org/10.5772/61024

ductile-matrix composite on fibre volume fraction V_f has a maximum. An inherent reason for decreasing composite strength at $V_f \geq V_f^{(max)}$ is arising a crack in the composite over a fibre cluster as a result of a single fibre break at a rather low stress followed by fracturing a number of adjacent fibres. The crack size arising because of fracture of a fibre cluster can be too large for the matrix to dissipate the elastic energy and arrest the crack. The probability of fibre cluster formation increases with the fibre volume fraction increases. A corresponding model of the composites failure behaviour was developed by Mileiko [1]. Recent experimental results revealing such behaviour of oxide-fibre/nickel-based matrix composites are published in [56]. A particular value of $V_f^{(max)}$ depends on fracture toughness of the matrix, fibre strength characteristics and a degree of non-homogeneity of fibre packing. Usually, for composites produced by infiltration of a fibre bundle with a matrix melt, $V_f^{(max)} < 0.3$ for room temperature behaviour because of a rather poor homogeneity of the fibre distribution in a specimen cross-section. Hence, the low strength of specimens at room temperature is characteristic of composites with larger fibre volume fraction and the same composites with $V_f < 0.3$ would definitely be characterised by a much higher strength.

Secondly, the strength of composites with V_f = 0.4 - 0.5 at room temperature and at 1200°C is approximately the same. Two factors contribute to this effect. First, this can be a result of high fibre/matrix interface strength, which results in loading the fibre to high stresses. The second factor is a shift of critical value V_f(max) of fibre volume fraction to higher values as a result of an increase in the matrix fracture toughness with temperature.

Composites of such a type are to be developed for high temperature use. Hence, creep properties of the composites are of importance. At a prelimary stage of the work described in [60] no creep tests have been performed yet, the results of strength tests together with a previous experience of the present author in studying creep of fibrous composites [51,52, 58] allow formulating some expectations. The theory of creep behaviour of MMCs [51] and a large bulk of the experimental data [56, 59, 60] show that the most important structural parameter of composites with oxide fibres produced via liquid infiltration route is the fibre/matrix interface strength determined by a degree of wetting in the system. If a matrix melt wets a fibre then the matrix heals the surface defects that yields an increase in the effective fibre strength by a factor as high as 5 in the case of a fibre obtained by the internal crystallisation method (see above Figure 13). The effective fibre strength determines creep resistance of composites at temperatures, at which fibre creep is negligible. The oxide fibres used in these experiments do not creep at a temperature of 1200°C (see Section 3). Also it is important to note that good wetting and, consequently, a strong interface make the basis of high creep resistance of the composites with large fibre volume fractions. Therefore, the composites described in short communication [56] can be expected to have a high creep resistance at temperatures to 1200°C.

6. Molybdenum-based composites reinforced with ICM-fibres

As was mentioned in Section 1 the development of refractory metal alloys for high temperature usage meets a problem in reaching an appropriate balance of three main characteristics of such alloys those being creep resistance, fracture toughness (damage tolerance), and oxidation resistance. Hence, the developments of fibrous composites with refractory alloy matrices can

obviously be considered as a way to overcome a problem of reaching the balance between creep resistance and fracture toughness. Recent results show a possibility to obtain such composites with an enhanced oxidation resistance [61, 62]. Measurements of oxidation resistance and creep properties were performed on specimens composed of unalloyed molybdenum matrix (containing 0.04% of impurities) and fibers of sapphire, single crystalline YAG and a number of alumina-garnets eutectics (Al_2O_3-$R_3Al_5O_{12}$ where R is Y, Yb or Tb). Three sets of the experiments were performed to evaluate oxidation resistance of the composites.

First, specimens of molybdenum and molybdenum-matrix composites reinforced with alumina-YAG eutectic and sapphire fibers of the same sizes were kept in air at a temperature of 1000°C for up to 1 h. A decrease in the mass of the specimens with time is plotted in Figure 31. A significant difference in the oxidation kinetics of molybdenum reinforced with the fibre containing yttrium compared to both pure molybdenum and molybdenum reinforced with sapphire fibre is obvious. Then the specimen reinforced with the Al_2O_3-$Y_3Al_5O_{12}$ eutectic fibre was exposed to a temperature of 1300°C for nearly 2 h. For comparison, a "fresh" pure molybdenum specimen was also tested. An essential difference in the oxidation of the composite and unreinforced pure molybdenum can be clearly seen. A hypothesis of formation of a sufficiently stable layer of yttrium molybdate on the composite surface attacked by oxygen can explain the result obtained.

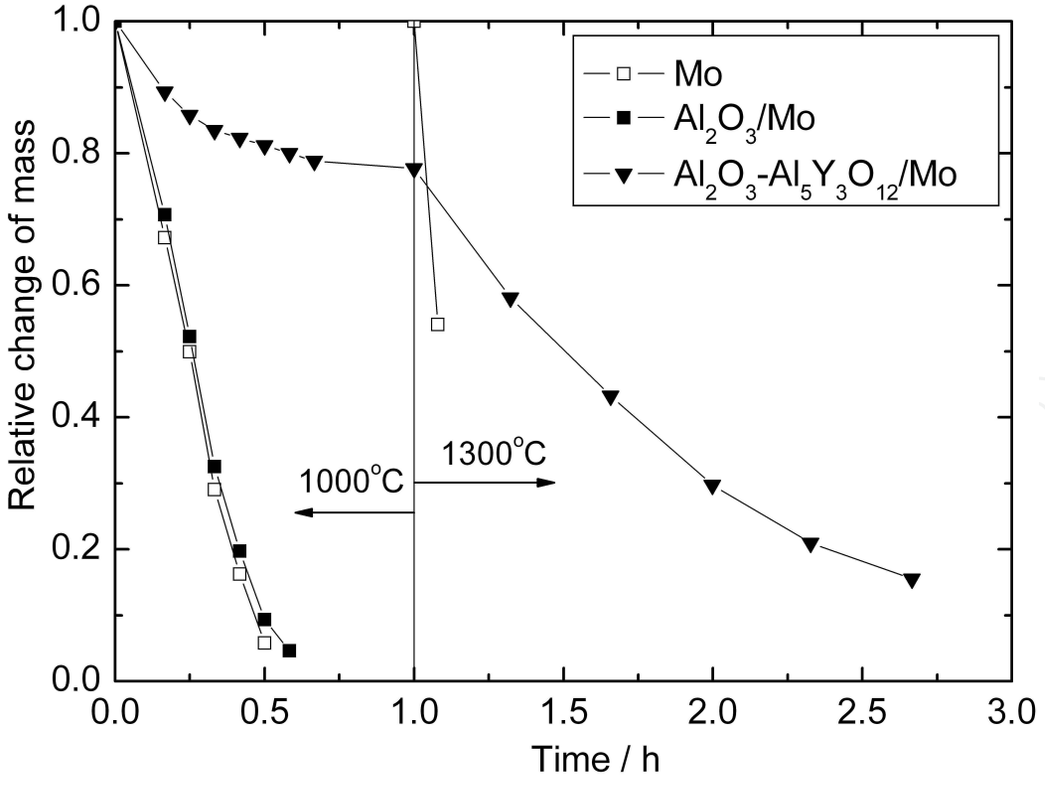

Figure 31. A relative decrease in the mass of molybdenum and oxide/molybdenum specimens with a surface of 20 cm^2 versus time of the exposure in air at 1000 and 1300°C.

http://dx.doi.org/10.5772/61024

The second series of the experiments was carried out to prove the hypothesis just formulated by a direct observation of the surface of a composite with molybdenum matrix and single crystalline YAG fibre heated in air at a temperature of 1000°C for 1 h. In Figure 32, one can see a fibre of a nearly tri-angular shape being originally single crystalline YAG. After heating, a layer in the fibre in a vicinity of the fibre/matrix interface occurs, which looks different from the centre of the fibre. The X-ray microanalysis was performed in three points marked on the micrograph. It was shown that (i) a chemical compound close to yttrium molybdate, $Y_2Mo_3O_{12}$ arises on the surface of both the molybdenum matrix and oxide fibre; (ii) the fibre has lost yttrium oxide and the composition of a layer arising near the interface is close to alumina. Examination of a specimen surface gives exactly the same result (Figure 33): The The X-ray microanalysis performed over areas 60X60 microns around points 4 – 6 shows that the surface is coated with a layer of the yttrium molybdate and depletion of yttria in the fibres is also observed. The only Y_2O_2-MoO_3 phase diagram published in 1982 and cited in [63] shows that the melting point of $Y_2Mo_3O_{12}$ is 1310°C and this sets a limitation for the usage of the composite.

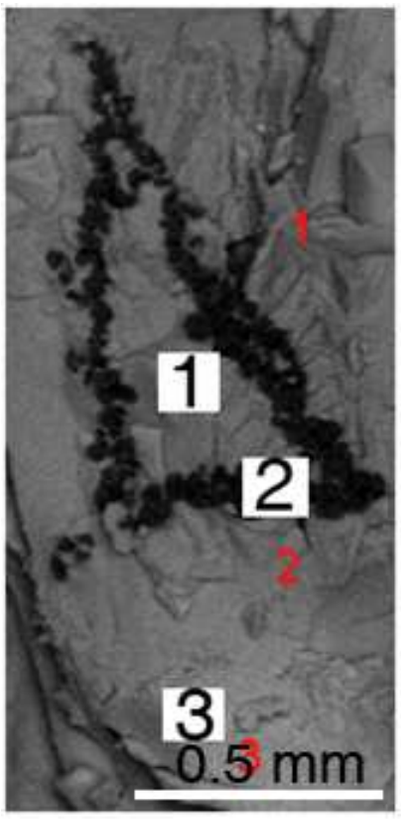

Figure 32. SEM micrograph of a face of a YAG-fibre/molybdenum-matrix specimen heated at 1000°C for 1 h.

Note that the specimens in this experiment had no coating, so a large quantity of yttria was withdrawn from the fibre exposed to a free surface. Obviously, a special coating will prevent molybdenum from oxidation and formation of the molybdate to heal possible defects in the coating will occur only in a vicinity of the damaged area of the coating.

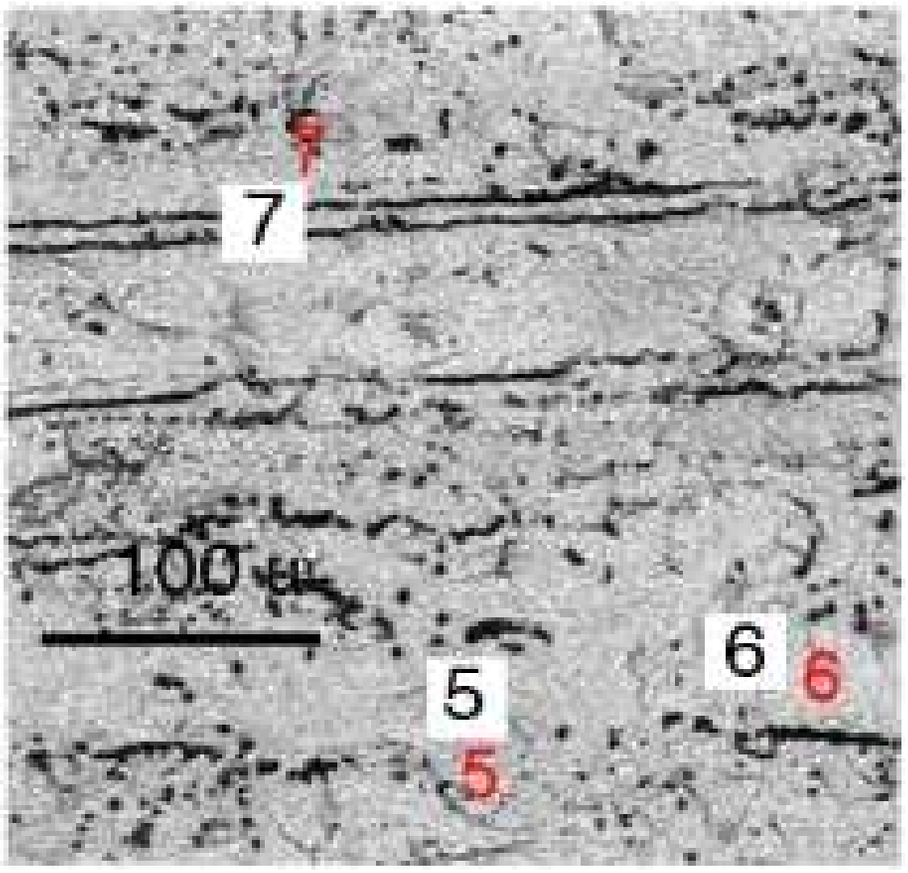

Figure 33. SEM micrograph of the sidepiece of a YAG-fibre/molybdenum-matrix specimen heated at 1000°C for 1 h.

The third set of the experiments was a study of oxidation kinetics of Mo-matrix composites with alumina-based eutectic fibres containing $Y_3Al_5O_{12}$, $Tb_3Al_5O_{12}$ and $Yb_3Al_5O_{12}$. Exposure temperature for these experiments was lower than in the first two sets, 700°C, and exposure time larger, up to 10 h. The oxidation kinetics is presented in Figure 34 together with that for pure molybdenum. The data for molybdenum is taken from reference [64]. It should be noted that those data have been obtained by exposing specimens in atmosphere with at a partial oxygen pressure of 76 mm Hg, which is much lower than that in normal air atmosphere. Still, the oxidation rates of the composites are much smaller.

A layer of a compound containing both molybdenum and yttrium is found on the surface of the specimen with Al_2O_3-$Y_3Al_5O_{12}$ eutectic fibres with atomic ratio Mo:Y ≈ 2:1, which corresponds to $Y_2Mo_4O_{15}$. Comparing this observation with the data obtained in the second set of the experiments leads to a hypothesis on the formation of a sequence of the molybdates with enhancing the exposure temperature. Nearly the same is found on the surface of a composite with eutectic fibers containing lanthanide elements. Again the Mo:Tb ratio is approximately 2. In the absence of published phase diagrams of a corresponding oxide system, it remains to expect an occurrence of $Tb_2Mo_4O_{15}$ on the specimen surface.

Tensile creep tests of the composites with Al_2O_3-$Y_3Al_5O_{12}$-eutectic fibre as model materials were conducted in vacuum at temperatures 1000 - 1300°C [27]. The dependence of rupture stress on

http://dx.doi.org/10.5772/61024

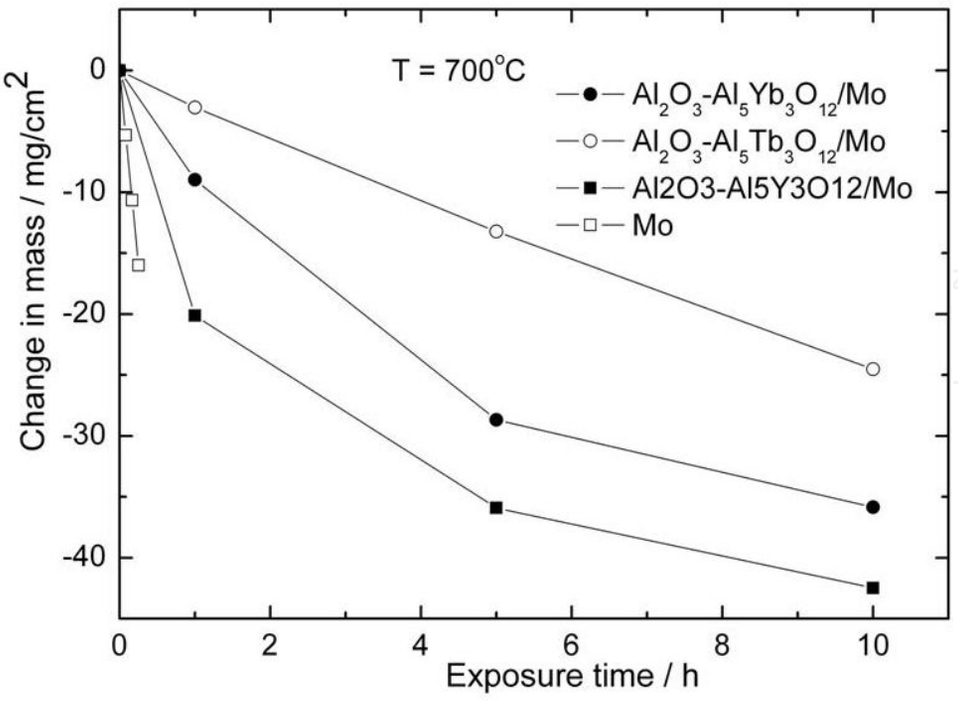

Figure 34. Oxidation kinetics at 700°C of three Mo-matrix composites with oxide fibers containing rare earth elements and that of unreinforced molybdenum. Experimental points for composites containing Al_2O_3-$Tb_3Al_5O_{12}$ and Al_2O_3-$Yb_3Al_5O_{12}$ eutectic fibres are the averages for three specimens. Those for composites containing Al_2O_3-$Y_3Al_5O_{12}$ fibres are the averages for six specimens.

time for temperature 1300°C is presented in Figure 35 together with the data acquired from experimental results published by Jain and Kumar [11], which describe creep rupture behaviour of molybdenum alloy of sufficiently high oxidation resistance. Creep rupture properties of the composite with a low density (~ 7.5 g/cm^3) on 100 h time base are better than those of the alloy. At lager rupture time the difference between values of the rupture stress for the composite and alloy will be even larger. This is because creep resistance of metal matrix composites with fibres of creep resistance much higher that of the matrix is determined by the fibre strength (see Eq. (5)) that yields a slop of the stress/time dependence in log-log coordinates for the composite much smaller than that for an alloy.

7. Prospects of the internal crystallisation method

The internal crystallisation method can be further developed to produce fibres and composites differ from those described in the previous sections. We limit ourselves just with two examples to illustrate the work in progress.

7.1. Composite oxide fibres

Fibrous composites containing inherently brittle matrix and brittle fibre can behave in a non-brittle manner provided a fibre/matrix interphase allows either fibre/matrix delamination or

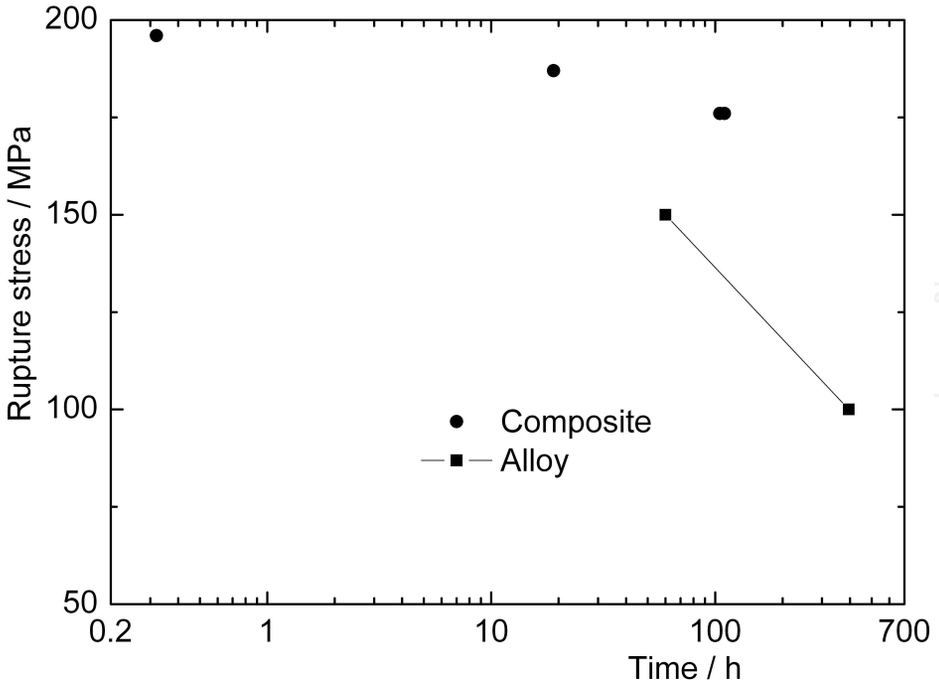

Figure 35. Creep strength of an Al_2O_3-$Y_3Al_5O_{12}$/Mo composite with fibre volume fraction of about 40% and that of most creep resistant three-phase Mo-Si-B alloy (acquired from experimental results in [11])

fibre pull-out. A usual way to organise such a kind of the "weak" interphase is to coat the fibre with an appropriate material. In the case of oxide-fibre/oxide-matrix composites, polycrystalline fibres, which are commercially available, are coated with either monazite or hexaaluminate type of the oxides [65, 66, 67]. Hexaaluminate $CaAl_{12}O_{19}$ (CA6 further on) has a hexagonal highly anisotropic structure, so that fracture-energy anisotropy reaches values of about 100 [71]. However, polycrystalline oxide fibres are creeping at rather low temperatures (see Figure 24), so the usage of single crystalline or eutectic fibres of the ICM type is wanted. Coating of ICM fibres is possible [68] but not a convenient procedure.

Therefore, a new design of the fibrous microstructure able to arrest cracks should be looking for. A possible solution is a composite oxide fibre containing a main ingredient, say sapphire, and a "weak" inclusion, say a kind of hexaaluminate, obtained by using the internal crystallization method [69]. To crystallise such fibres, raw mixtures of oxides containing 2 – 3 – 4.5 – 6 mass per cent of calcia in alumina were prepared to be used in the ICM process. Pulling rate of the oxide/molybdenum blocks varied from less than 1 mm/min to 800 mm/min. In the first experiment, just to show a possible microstructure of hexaaluminate, pure CA6, without alumina was crystallised, the result is presented in Figure 36. It can be seen that the flat surface of the fibre is coincided with the basis crystallographic plane of CA6. Also it is obvious that the fibre is not single crystalline and the fibres of such type cannot be sufficiently strong.

Composites with Al_2O_3-$CaAl_{12}O_{19}$ fibre and brittle molybdenum matrix (molybdenum in a block shown in Figure 3 is brittle being fully recrystallised) demonstrate quasi-plastic behaviour as can be seen in Figure 37a. Fracture surface (Figure 37b) of a composite specimen of the same type reveals fibre pull out.

http://dx.doi.org/10.5772/61024

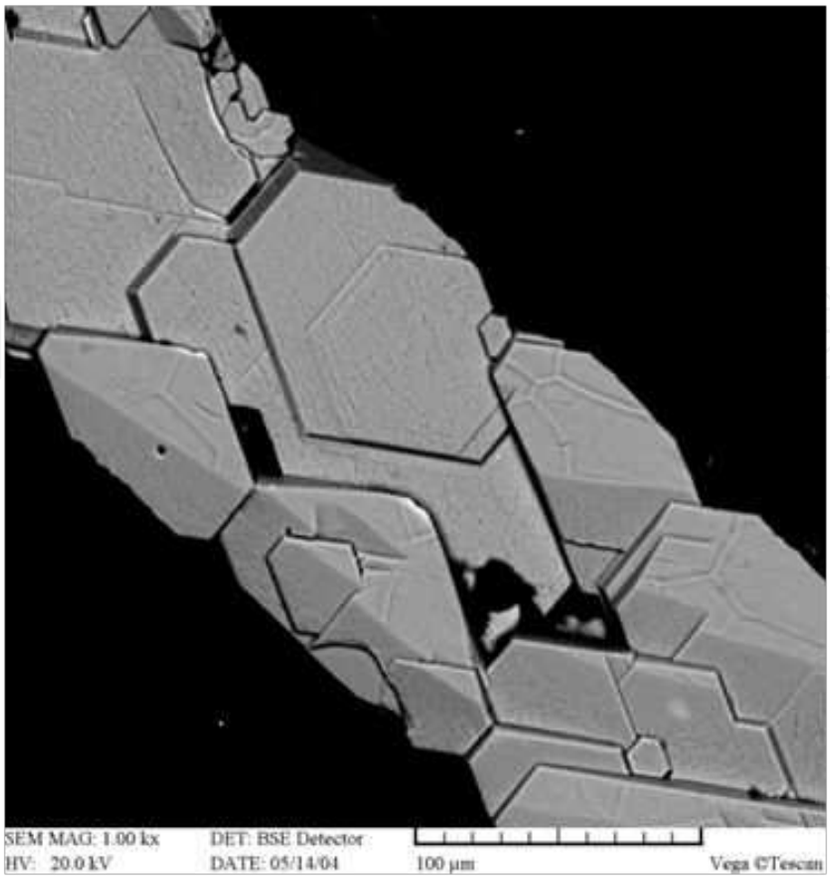

Figure 36. A flat surface of the fibre made of pure hexaaluminate.

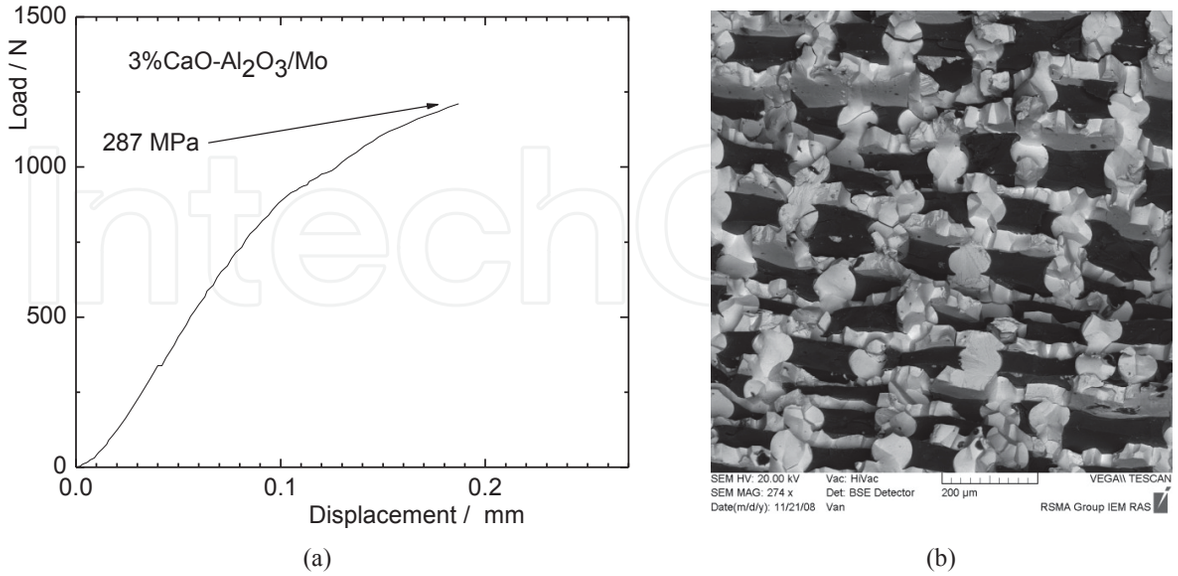

Figure 37. Load/displacement curve of a composite with brittle molybdenum matrix under 3-point bending (a); Failure surface of similar specimen with a fibre obtained from raw mixture Al_2O_3+2%CaO at pulling rate of 1 mm/min.

Hence, there is a hope to develop composite oxide fibres to be an effective reinforcement for brittle matrix.

7.2. Silicide-fibre/molybdenum-matrix composites

As shown in Section 1 a mainstream in the development of heat resistant materials beyond nickel superalloys is searching for molybdenum alloy with a necessary balance of three main characteristics, those being creep resistance, damage tolerance and oxidation resistance. A goal to develop an alloy with the use temperature as high as 1300°C is expected to be reached by introducing into molybdenum matrix brittle particles of complex silicides. However, the alloys with sufficiently high creep and oxidation properties remain to be optimized to satisfy damage tolerance requirement. At the same time, it was mentioned in Section 1 that reinforcing a ductile metal matrix with brittle fibre can lead to a composite of an enhanced fracture toughness properties. Hence, it is interesting to look at prospects of the internal crystallization method to make silicide-fibre/refractory-metal-matrix composites. Preliminary experiments with silicide-fibre/molybdenum-matrix composites were conducted recently [70].

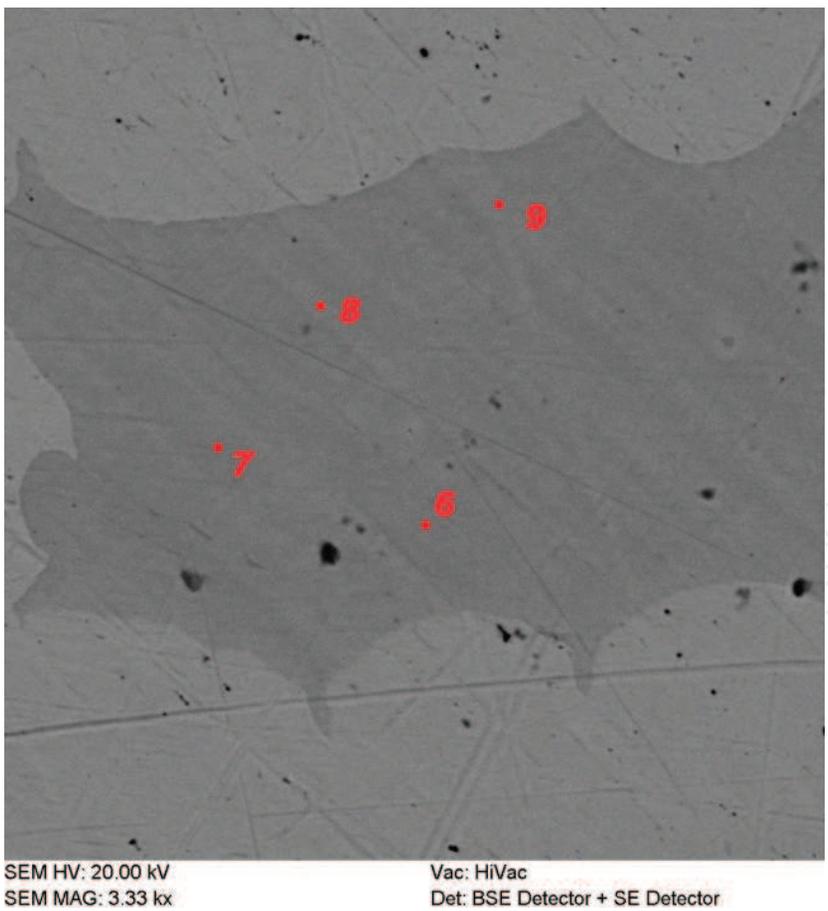

Figure 38. A typical microstructure of the molybdenum-silicide-fibre/molybdenum-matrix composite.

http://dx.doi.org/10.5772/61024

A most difficult couple of the ingredients to deal with is a molybdenum carcass and molybdenum disilicide, $MoSi_2$, with the melting temperature 2020°C and this couple was chosen for the first experiments. The $MoSi_2$ melt was expected to interact with molybdenum to form silicides with a larger content of Mo, Mo_5Si_3 or even Mo_3Si. In fact, the $MoSi_2$ -melt/molybdenum interaction yields a drastic change in the fibre shape and its composition. The fibre lost its plane surfaces, Figure 38, they show traces of a complicated process of the chemical interactions. The Mo:Si atomic ratio measured in the points marked in the area of the fibre is about 3.4, which is close to silicide Mo_3Si. The The X-ray microanalysis of the matrix reveals a presence of silicon, certainly in the form of inclusions of Mo_3Si of small size since the The X-ray spectrum obtained from a cross-section of a specimen (Figure 39) shows only molybdenum and Mo_3Si.

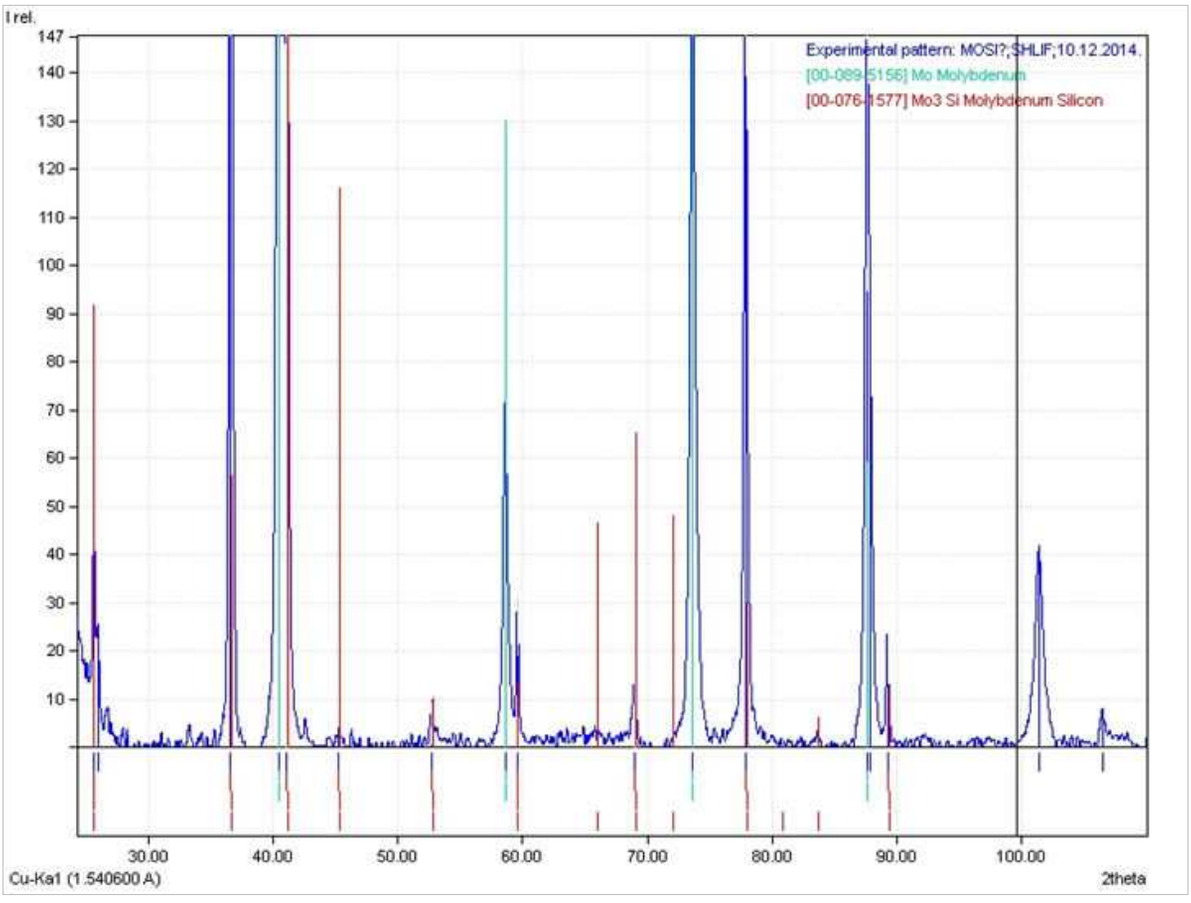

Figure 39. The X-ray spectrum obtained from a cross-section section of the molybdenum-silicide-fibre/molybdenum-matrix specimen.

Creep tests of specimens were conducted in bending at a temperature of 1410°C and the results of the experiments were interpreted on the basis of the method outlined above. One specimen was tested under a step-wise changing of the load, and the value of n occurred to be around 5. All the data were obtained by assuming $n = 5$; they are presented in Figure 40.

It is important to note that value of $n = 5$ was evaluated for a composite with fibre volume fraction $V_f = 0.2$. Because the value of n increases with V_f increasing (see Figure 25, in which the exponent was denoted as q), the value of creep resistance for composites with V_f different from 0.2, which were calculated assuming $n = 5$, are to be corrected as shown in Figure 40 by the arrows. This would make the dependence of the creep resistance for fibre volume fraction close to linear, which is characteristic for composites with a strong fibre/matrix interface.

Therefore the preliminary data just described show that the ICM is a prospective way to obtain silicide fibrous composites.

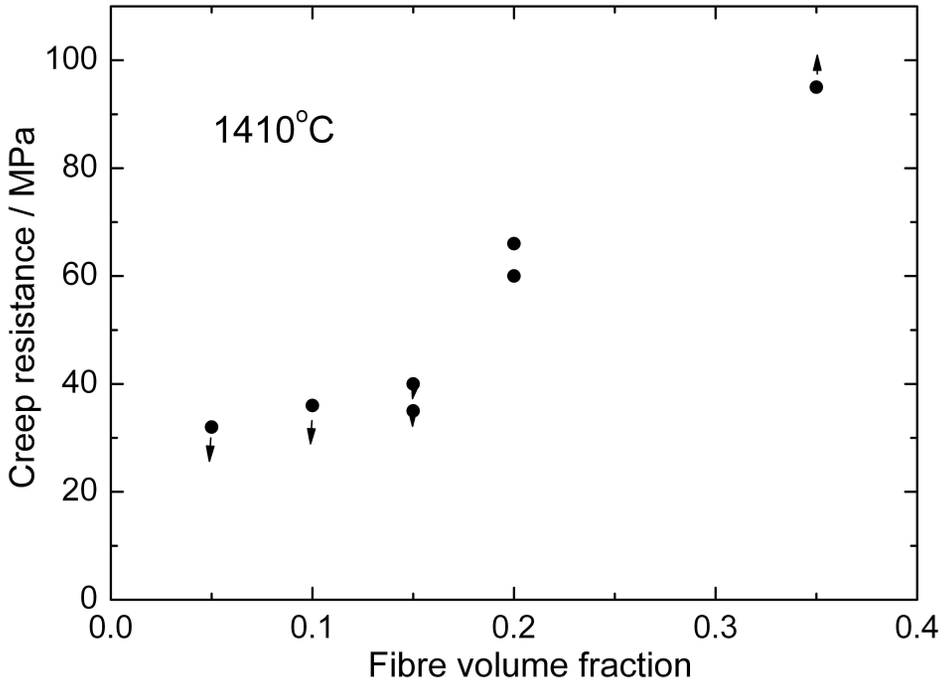

Figure 40. Creep resistance at 1410°C of Mo_3Si-Mo composites versus fibre volume fraction.

8. Conclusions

1. The internal crystallisation method (ICM) can be a base for developing effective technologies to produce a large family of oxide fibres with mechanical properties similar to those of the fibres produced by using traditional methods.

2. ICM-fibres can be used to obtain heat resistant composites with a number of the matrices including nickel superalloys and recently invented high entropy alloys.

3. An appropriate choice of the chemical composition of oxide reinforcements for refractory matrices can be a way to reach a necessary balance of the main properties of heat resistant materials, those being creep resistance, fracture toughness and oxidation resistance.

4. Composite ICM-fibres containing highly anisotropic oxide inclusions can be an effective reinforcements for brittle matrices to produce non-brittle composites.

5. Silicide fibrous reinforcements can also be produced by using ICM.

Acknowledgements

New results reported in the present chapter have been obtained in the framework of projects supported by Russian Foundation for Basic Research (## 13-08-90459, 14-08-01254 and 15-03-05415). The author is thankful to his colleagues who worked hard even in the difficult for Russian science times, years 1990-2005. Special thanks to Drs A.V. Serebryakov, V.I. Kazmin, A.A. Khvostunkov, V.V. Tvardovsky, N.I. Novokhatskaya, A. M. Rudnev and A.N. Tolstun, Mrs. N.A. Prokopenko, Mr. L.S. Kozhevnikov, Mr. A.Ya. Mizkevich, Mr. A.A. Kolchin, Mr. V.A. Chumichev, Mr. D.G. Pizhenin. Regrettably, some of them (AVS, VIK, AAKh and LSK) have passed away..

Author details

Sergei T. Mileiko

Address all correspondence to: mileiko@issp.ac.ru

Institute of Solid State Physics of RAS, Moscow, Russia

References

[1] Mileiko ST. Metal and Ceramic Based Composites. Amsterdam: Elsevier; 1997. 702 p. ISBN: 978-0-444-82814-9

[2] Logunov AV, ShmotinYuN. Advanced heat resistant nickel alloys for gas turbine disks. Nauka I Techologii: Moscow; 2013. 256 p. (in Russian).

[3] Naslain R. Fibrous ceramic-ceramic composite materials processing and properties.Journal de Physique. 1986;47:C1-703-715. DOI: 10.1051/jphyscol:19861107

[4] GE9X - GE Aviation. Available from: http://www.geaviation.com/newengine/ Accessed: 2015-06-02

[5] Lange FF, Tu WC, Evans AG.Processing of damage-tolerant, oxidation-resistant ceramic matrix composites by a precursor infiltration and pyrolysis method. Mater Sci-Eng A. 1995;195:145–150. DOI:10.1016/0921-5093(94)06513-6

[6] Zok FW.Developments in oxide fiber composites. J Am Ceram Soc. 2006;89:3309–3324. DOI: 10.1111/j.1551-2916.2006.01342.x

[7] Volkmann E, Tushtev K, Koch D, Wilhelmi C, Göring J, Rezwan K. Assessment of three oxide/oxide ceramic matrix composites: Mechanical performance and effects of heat treatments. Composites Part A. 2015;68:19–28. DOI: 10.1016/j.compositesa.2014.09.013

[8] Grammenos I, Tsakiropoulos P. Study of the role of Hf, Mo and W additions in the microstructure of Nb-20Si silicide based alloys. Intermetallics. 2011;19: 1612-1621. DOI:10.1016/j.intermet.2011.06.008

[9] US Patent 7,704,335 published April 27, 2010.

[10] Tanaka R, Kasama A, Fujikura M, Iwanaga I, Tanaka H, Matsumura Y. Research and development of niobium-based superalloys for hot components of gas turbines. In: Proceedings of International Gas Turbine Congress; 2-7 November 2003; Tokyo: p.1-5

[11] Jain V, Kumar K S. Tensile creep of Mo–Si–B alloys.Acta Mater.2010; 58:2124–2142.DOI:10.1016/j.actamat.2009.11.054

[12] Heilmaier M, Krüger M, Saage H, Rösler J, Mukherji D, Glatzel U, Völkl R, Hüttner R, Eggeler G, SomsenCh, Depka T. Metallic materials for structural applications beyond nickel-based superalloys. J. Metals.2009; 61:61-67. DOI: 10.1007/s11837-009-0106-7

[13] Lemberg J .A, Middlemas M R, Weingärtner T, Gludovatz B, Cochran J K, Ritchie R O. On the fracture toughness of fine-grained Mo-3Si-1B (wt.%) alloys at ambient to elevated (1300oC) temperatures. Intermetallics. 2012; 20;141-154. DOI:10.1016/j.intermet.2011.09.003

[14] LaBelle H E, Jr, Mlavsky A I. Growth of sapphire filaments from the melt. Nature; 1967; 216:574-575. DOI:10.1038/216574b0

[15] Stepanov AV.A Future of Metal Processing. Leningrad: Machinostroenie; 1963 (in Russian).

[16] Mileiko S T. Oxide fibres. In: Watt WW and Perov BV, eds. Strong Fibres, Handbook of Composites. Vol. 1. Amsterdam: North-Holland; 1985. p. 87- 114.ISBN-13: 978-0444875051 ISBN-10: 0444875050

[17] Fukuda T, Chani V I, editors, Shaped Crystals Growth by Micro-Pulling-Down Technique. Berlin Heidelberg: Springer-Verlag; 2007. ISBN: 3540712941

[18] Burrus C A, Coldren L A. Growth of single-crystal sapphire-clad ruby fibers.Appl-PhysLett 1977; 31:383-384.DOI:org/10.1063/1.89713

[19] Feigelson S H, Kway W L, Route R K. Single crystal fibers by the laser-heated pedestal growth method. Optical Engineering.1985; 24:822-830. doi:10.1117/12.7973637

[20] Haggerty J S, Wills K S, Sheehan J E. Growth and properties of single crystal oxide fibers. In: Proceedings of the 15th Annual Conference on Composites and Advanced Ceramic Materials, Part 2 of 2: Ceramic Engineering and Science Proceedings, Volume 12, Issue 9/10; 1991; p. 1785-1801 DOI: 10.1002/9780470313848.ch13

[21] Shahinian P. High-temperature strength of sapphire filaments. J Amer Ceram Soc. 1971;54:67-68. DOI:10.1111/j.1151-2916.1971.tb12180.x

[22] Hurley GF.Short-term elevated temperature tensile behaviour in 0o sapphire filaments. J Mater Sci 1972;7:471-473.

[23] Kotchick DM, Hink RC, Tressler RE. Gauge length and surface damage effects on the strength distributions of silicon carbide and sapphire filaments. J Compos Mater 1975; 9:327-340.

[24] Newcomb SA, Tressler RE.High-temperature fracture toughness of sapphire, J Am Ceram Soc. 1994; 77:3030-3032.DOI: 10.1111/j.1151-2916.1994.tb04542.x

[25] Mileiko ST, Kazmin VI. Crystallization of fibres inside a matrix: a new way of fabrication of composites. J Mater Sci. 1992; 27: 2165-2172.DOI: 10.1007/BF01117932

[26] Mileiko ST, Kazmin VI. Structure and mechanical properties of oxide fibre reinforced metal matrix composites produced by the internal crystallization method. CompSci Tech. 1992; 45:209-220. DOI:10.1016/0266-3538(92)90081-D

[27] KurlovVN, KiikoVM, Kolchin AA, Mileiko ST. Sapphire fibres grown by a modified internal crystallization method.J Crystal Growth.1999; 204:499-504.DOI: 10.1016/S0022-0248(99)00213-4

[28] Mileiko ST, Kiiko VM, Sarkissyan NS, StarostinMYu, Gvozdeva SI, Kolchin AA, Strukova GK. Microstructure and properties of Al2O3-Al5Y3O12 fibre produced via internal crystallization route. Compos Sci Tech. 1999; 59:1763-1772; DOI: 10.1016/S0022-0248(99)00213-4

[29] Mileiko ST, Kurlov VN, Kolchin AA, Kiiko VM.Fabrication, properties and usage of single-crystalline YAG fibres.Journal of the European Ceramic Society.2002; 22:1831-1837.DOI:10.1016/S0955-2219(01)00505-2

[30] Rüscher CH, Mileiko ST, Schneider H. Mullite single cyrystalfibers produced by the internal crystallization method (ICM). Journal of the European Ceramic Society.2003; 23: 3113–3117.DOI:10.1016/S0955-2219(03)00118-3

[31] Mileiko ST. Single crystalline oxide fibres for heat-resistant composites. Compos.Sci. and Technol. 2005; 65: 2500-2513.DOI: 10.1016/j.compscitech.2005.05.029

[32] Mileiko ST, Serebryakov AV, Kiiko VM, Kolchin AA, Kurlov VN, Novokhatskaya NI,Tolstun AN. Single crystalline mullite fibres obtained by the internal crystallisation method. Composites and Nanostructures, 2009; #2: 47-46 (in Russian).

[33] Mileiko ST, Serebryakov AV, Kiiko VM, Kolchin AA, Kurlov VN, Novokhatskaya NI. Single crystalline mullite fibres obtained by the internal crystallisation method:

microstructure and creep resistance. J Europ Ceram Soc. 2009; 29: 337-345.DOI: 10.1016/j.jeurceramsoc.2008.06.022

[34] Mileiko ST, Kiiko VM, Novokhatskaya NI,Tolstun AN, Kolchin AA. Single crystalline fibres of yttrium-aluminium garnet: microstructure and room temperature strength. Deformation and Fracture of Materials.2008; #5: 2-7 (in Russian).

[35] Dokko PC, Pask JA, Mazdiyasni KS.High-temperature mechanical properties of mullite under compression. J. Am. Ceram. Soc. 1977; 60: 150-155DOI: 10.1111/j.1151-2916.1977.tb15492.x

[36] Kriven WM, Palko JW, Sinogeikin S, Bass JD, Sayir A, Brunauer G, Boysen H, Frey F, Schneider J. High temperature single crystal properties of mullite, J European Ceramic Society.1999;19:2529-2541.DOI: 10.1016/S0955-2219(99)00124-7

[37] Pask JA.Importance of starting materials on reactions and phase equilibria in the AI2O3-Si02 system. J. European Ceram. Soc. 1996; 16: 101-108.DOI: 10.1016/0955-2219(95)00147-6

[38] Mileiko ST, Kiiko VM, StarostinM.Yu, Kolchin AA, Kozhevnikov L.S. Fabrication and some properties of single crystalline mullitefibers. ScriptaMaterialia. 2002; 22:1831–1837.DOI: 10.1016/S0955-2219(01)00505-2

[39] Tolstun AN, Kiiko VM, Kolchin AA, Kurlov VN, Novokhatskaya NI, Mileiko ST. Fabrication, microstructure and high temperature mechanical propertyies of some oxide eutectic fibres. Deformation and Fracture of Materials. 2007; #3: 12-20 (in Russian).

[40] Mileiko ST, Sarkissyan NS, Kolchin AA, Kiiko VM. Oxide fibres in a Ni-based matrix – do they degrade or become stronger? Journal of Materials:Design and Applications. 2004; 218:193-200.DOI: 10.1177/146442070421800303

[41] Kiiko VM, Mileiko ST. Evaluation of room temperature strength of oxide fibres produced by the internal crystallization method.Compos.Sci. and Technol. 1999; 59:1977-1981.DOI:10.1016/S0266-3538(99)00054-8

[42] Mileiko ST. Oxide-fibre/Ni-based matrix composites – III: A creep model and analysis of experimental data.Compos Sci Tech. 2002; 62:195-204.DOI: 10.1016/S0266-3538(01)00162-2

[43] RabotnovYuN, Mileiko ST. Short-Time Creep. Moscow: Nauka Publishers. 1970 224 p. (in Russian).

[44] Corman GS.High-temperature creep of some crystal oxides. Proceedings of the 15th Annual Conference on Composites and Advanced Ceramic Materials, Part 2 of 2: Ceramic Engineering and Science Proceedings, Volume 12, Issue 9/10: p. 1745-1766. DOI: 10.1002/9780470313848.ch10

[45] Harada Y, Suzuki T, Hirano K, Waku Y.Ultra-high temperature compressive creep behavior of an in-situ Al2O3 single-crystal/YAG eutectic composite. JEuropeanCeramSoc. 2004; 24:2215-2222.DOI:10.1016/S0955-2219(03)00640-X

[46] Mileiko ST, Kazmin VI.Fabrication of composites by the internal crystallization method.MechanicaCompositnychMaterialov. 1991; #5:898-908 (in Russian).

[47] Wilson DM, Visser LR.High performance oxide fibers for metal and ceramic composites.Composites Part A:2001; 32:1143–1153. DOI:10.1016/S1359-835X(00)00176-7

[48] Mileiko ST. Speeding up creep tests of novel high temperature composites. In: Proceedings of 15th International Conference on Experimental Mechanics (ICEM-15). 22-27 July 2012; Porto: INEGI; 2012. P. 13-14.

[49] AsthanaR, Tewari SN, Draper SL. Strength degradation of sapphire fibers during pressure casting of a sapphire-reinforced Ni-base superalloy.Metallurgical and Materials Transactions A: Physical Metallurgy and MaterialsScience. 1998; 29A:1527-1530. DOI: 10.1007/s11661-998-0370-0

[50] Asthana R, Mileiko ST, Sobczak N. Wettability and interface considerations in advanced heat-resistant Ni-based composites. Bulletin of the Polish Academy of Sciences, Technical Sciences.2006;54:147-166.

[51] Mileiko ST, Kiiko VM, Kolchin AA, Serebryakov AV, Korzhov VP, Starostin My, Sarkissyan NS. Oxide-fibre/Ni-based matrix composites – I: Fabrication and microstructure, Compos. Sci. and Technol. 2002; 62:167-179.DOI:10.1016/S0266-3538(01)00197-X

[52] Novokhatskaya NI, Tolstun AN, Kiiko VM, Kolchin AA, Mileiko ST.An effect of non-homogeneous fibre packing on mechanical properties of oxide/nickel composites.Composites and Nanostructures, 2011; #1:5-17 (in Russian).

[53] Yeh JW, Chen SK, Lin SJ, Gan JY, Chin TS, Shun TT, Tsau CH, Chang SY. Nanostructured high-entropy alloys with multiple principal elements: Novel alloy design concepts and outcomes. Adv Eng Mater 2004; 6:299–303. DOI: 10.1002/adem.200300567

[54] Zhang Y, Zhou YJ.Solid Solution Formation Criteria for High Entropy Alloys.Materials Science Forum. 2007; 561-565:1337-1339. DOI: 10.4028/www.scientific.net/MSF.561-565.1337

[55] Liu CM, Wang HM, Zhang SQ, Tang HB, Zhang AL. Microstructure and oxidation behaviour of new refractory high entropy alloys. J Alloys Compounds 2014; 583:162–169. DOI: 10.1016/j.jallcom.2013.08.102

[56] Mileiko ST, Firstov SA, Novokhatskaya NI, Gorban' VF, Krapivka NP.Oxide-fibre/high-entropy-alloy-matrix composites. Composites Part A 2015;76:131-134. 10.1016/j.compositesa.2015.05.023

[57] Firstov SA, Gorban VF, Krapivka NA, Pechkovsky EP, Samilyuk AV. High temperature mechanical properties of cast nano-structured high entropy alloys. In: Proceed-

ings of 4th Intern Conf Deformation and Fracture of Materials and Nanomaterials, Moscow: IMET RAS, 2011 p 396-398.

[58] Mileiko ST. Steady state creep of a composite material with short fibres.1970; 5:254-261. DOI: 10.1007/BF00551002

[59] Mileiko ST, Kiiko VM, Kolchin AA, Korzhov VP, Prokopenko VM, Oxide-fibre/Ni-based matrix composites – II: Mechanical behaviour. Compos.Sci. and Technol. 2002, 62:181-193. DOI: 10.1016/S0266-3538(01)00161-0

[60] Mileiko ST, Kiiko VM, Kolchin AA, Novokhatskaya NI, Van KV, Bazyleva OA, BondarenkoYu.A. Creep of oxide/nickel composites. Composites and Nanostructures. 2009; №4:5-18 (in Russian).

[61] Mileiko ST, Novokhatskaya NI.On a possibility to make heat resistant composites of high gas corrosion resistance based on refractory metal matrix. Composites and Nanostructures.2012; # 4:5-14 (in Russian).

[62] Mileiko ST, Novokhatskaya NI.High temperature oxide-fibre/molybdenum-matrix composites of improved oxidation resistance, Journal of Materials Engineering and Performance.DOI: 10.1007/s11665-014-1305-0

[63] Phase Equilibria Diagrams, Acer – NIST, Version 3, CD-ROM Database (2003).

[64] MorgunovaNI, Klypin BA, Boyarshinov VA, Tarakanov LA, ManeginYu.A. Molybdenum alloys. Moscow: Metallurgia (1975), in Russian.

[65] Evans AG, Zok FW.The physics and mechanics of fibre-reinforced brittle matrix composites.J Mater.Sci. 1994; 29: 3857 – 3896. DOI: 10.1007/BF00355946

[66] Zok FW.Developments in Oxide Fiber Composites.J. Am. Ceram. Soc.2006; 89:3309–3324. DOI: 10.1111/j.1551-2916.2006.01342.x

[67] M. K. Cinibulk, Hexaluminates as a cleavable fiber-matrix interphase: synthesis, texture development, and phase compatibility.Journal of the European Ceramic Society. 2000; 20:569-582.DOI:10.1016/S0955-2219(99)00255-1

[68] PopovaNA, TolstunAN. FormationofmonaziteinterphaseinoxideoxidecompositeswithICM-fibres.SciencetoIndustry. 2007;#2:58-61 (in Russian).

[69] Mileiko ST, Kolchin AA, Novokhatskaya NI, Kiiko VM, Novikov IV.Quasi-plastic behaviour of brittle-matrix composites with oxide composite fibres. In: Proceedings of 16th European Conference on Composite Materials. Seville: July 2014.

[70] Mileiko ST, Novokhatskaya NI, Stolin AM, Bazhin PM. Producing silicide/molybdenum composites by using internal crystallization method. Composites and Nanostructures.2014; 6:185-197 (in Russian).